

RESEARCH ARTICLE

Open Access



Cranial and endocranial comparative anatomy of the Pleistocene glyptodonts from the Santiago Roth Collection

Zoe M. Christen¹, Marcelo R. Sánchez-Villagra¹ and Kévin Le Verger^{1*}

Abstract

With their odd cranial features, glyptodonts, closely related to extant armadillos, are a highly diverse group of the South American megafauna. *Doedicurus*, *Glyptodon*, *Panochthus*, and *Neosclerocalyptus* were present in the “Pampean Formation” during the Pleistocene, and they are all exceptionally preserved in the Santiago Roth Collection, thus offering the possibility of investigating these four well-diversified genera. A total of 13 specimens (seven species) were analysed and compared in a qualitative/quantitative study of external cranial remains and endocranial reconstructions (i.e., braincase and associated cranial canals, and inner ears). We report on anatomical features that contribute to existing phylogenetic matrices; many of them are new potential synapomorphies supporting the current hypotheses regarding the evolutionary history of the Pleistocene glyptodonts. These include the anterior cranial shape, the position of the basicranium in respect to the whole cranium, the shape of the cranial roof, the position of the largest semicircular canal, and the inclination of the cerebrum. They may represent new shared-derived features among *Glyptodon*, *Doedicurus*, *Neosclerocalyptus*, and *Panochthus*. We also provide detailed comparative descriptions highlighting new potential convergences in respect to current phylogenies, concerning, for instance, the shape of the foramen magnum, the global shape of the cranium, orbital shape, cochlear position, and a strong protrusion of the zygomatic process of the squamosal. In light of these results, we discuss morphological transformations across phylogeny. The endocranial comparison brought insights on the phylogenetic patterns of cranial canal evolution.

Keywords Pampean Region, Phylogeny, Convergence, Endocast, Inner ear, Morphometrics

Resumen

Con sus extrañas características craneales, los gliptodontes, estrechamente emparentados con los armadillos vivientes, constituyen un grupo muy diverso de la megafauna sudamericana. *Doedicurus*, *Glyptodon*, *Panochthus* y *Neosclerocalyptus* estuvieron presentes en la “Formación Pampeana” durante el Pleistoceno, y todos ellos están excepcionalmente conservados en la Colección Santiago Roth, ofreciendo así la posibilidad de investigar estos cuatro géneros muy diversificados. Se analizaron y compararon un total de 13 especímenes (cuatro géneros; siete especies) en un estudio cualitativo/cuantitativo de la anatomía extracraneana y endocraneana (es decir, el encéfalo, los conductos craneanos asociados y el oído interno). Informamos sobre rasgos anatómicos que pueden contribuir a las matrices

Editorial handling: Analía M. Forasiepi

*Correspondence:

Kévin Le Verger

kevin.leverger@pim.uzh.ch

Full list of author information is available at the end of the article



© The Author(s) 2023. **Open Access** This article is licensed under a Creative Commons Attribution 4.0 International License, which permits use, sharing, adaptation, distribution and reproduction in any medium or format, as long as you give appropriate credit to the original author(s) and the source, provide a link to the Creative Commons licence, and indicate if changes were made. The images or other third party material in this article are included in the article's Creative Commons licence, unless indicated otherwise in a credit line to the material. If material is not included in the article's Creative Commons licence and your intended use is not permitted by statutory regulation or exceeds the permitted use, you will need to obtain permission directly from the copyright holder. To view a copy of this licence, visit <http://creativecommons.org/licenses/by/4.0/>.

filogenéticas existentes; muchos de ellos son nuevas sinapomorfías potenciales que apoyan las hipótesis filogenéticas actuales de los gliptodontes del Pleistoceno. Entre ellas se encuentran la forma craneal anterior, la posición del basicráneo respecto al conjunto del cráneo, la forma del techo craneano, la posición del canal semicircular mayor y la inclinación del encéfalo. Éstos pueden representar nuevos rasgos derivados para *Glyptodon*, *Doedicurus*, *Neosclerocalyptus* y *Panochthus*. También proporcionamos una descripción comparativa detallada destacando nuevas convergencias potenciales con respecto a las filogenias actuales, relativas, por ejemplo, a la forma del foramen magnum, la forma general del cráneo, la forma orbital, la posición coclear y una fuerte protrusión del proceso cigomático del escamoso. A la luz de estos resultados, discutimos las transformaciones morfológicas a lo largo de la filogenia. La comparación endocraneana aportó información sobre los patrones de los canales craneanos en un contexto filogenético.

Palabras clave Región Pampeana, Filogenia, Convergencia, Molde endocraneano, Oído interno, Morfometría

Introduction

Glyptodonts are among the most emblematic representatives of the extinct South American megafauna. In the Pleistocene, they exhibited a relatively high diversity, before becoming extinct in the Early Holocene (Barnosky & Lindsey, 2010; Prado et al., 2015). Since the first classification works (e.g., Ameghino, 1897; Burmeister, 1866; Cuvier, 1798; Gray, 1869; Huxley, 1864; Owen, 1839a; Trouessart, 1897), the presence of osteoderms covering the whole body from head to tail represents an evident synapomorphy grouping the glyptodonts and the extant armadillos. In addition to several skeletal features, these gigantic herbivores, some weighing up estimated two tons (Vizcaíno et al., 2011), were distinguished by an immobility of the dorsal carapace and, more distinctly, by the acquisition of cranial features so derived that they were judged as the clade with the oddest anatomy of all mammals (Burmeister, 1874; Carlini & Zurita, 2010; Vizcaíno & Loughry, 2008). Based on molecular data, the hypothesis of their inclusion within the armadillos was reinforced with a phylogenetic position as the sister-group of the clade Chlamyphorinae + Tolypeutinae (Delsuc, 2016; Mitchell et al., 2016). Their large size coupled with the presence of osteoderms led them to be among the most abundant mammals in the South American fossil record (e.g., Le Verger, 2023; Vizcaíno & Loughry, 2008). Pleistocene Glyptodontidae are mainly represented by four genera, *Glyptodon* Owen, 1839b, *Doedicurus* Burmeister, 1874, *Neosclerocalyptus* Paula Couto, 1957, and *Panochthus* Burmeister, 1866 (e.g., Carlini & Scillato-Yané, 1999; Cuadrelli et al., 2019; Zurita et al., 2011a).

The abundance of the fossil record of glyptodonts is partly due to the quantity of osteoderms of a single carapace. This abundance in addition to osteoderm variation has led to an overestimation of glyptodont diversity, especially during the Pleistocene (e.g., McKenna & Bell, 1997; Fornicola & Porpino, 2012). The reassessments of glyptodont diversity during the last ten years have been confined more largely within genera or subfamilies than

among them (e.g., Cuadrelli et al., 2020; Núñez-Blasco et al., 2021; Zamorano et al., 2014a; Zurita et al., 2018). For instance, according to Cuadrelli et al. (2020), *Glyptodon* is composed of only three species *Glyptodon munizi* Ameghino, 1881, *Glyptodon reticulatus* Owen, 1845, and *Glyptodon jatunkhirki* Cuadrelli, Zurita, Toriño, Miño-Boilini, Perea, Luna, Gilette & Medina, 2020, which marks a drastic decrease in the traditionally assumed diversity of *Glyptodon* during the Pleistocene (McKenna & Bell, 1997; Zurita et al., 2018). Another good example of taxonomical reduction concerns *Neosclerocalyptus*, due to many erroneous interpretations and assignments to "Lomaphorini" and *Hoplophorus* Lund, 1839 based on taphonomic alterations (Quiñones et al., 2020; Zurita et al., 2017). This genus is composed of only four species during the Pleistocene (Zurita et al., 2011b). The opposite is shown when dealing with the diversity of *Panochthus*, where a taxonomic expansion is observed during the Late Pleistocene with currently eight species included in the genus (Zamorano et al., 2021). Concerning the Doedicurinae, only one Pleistocene species, *Doedicurus clavicaudatus* Gervais & Ameghino, 1880, is well-established, but several authors proposed an intense taxonomic revision of this clade (e.g., Núñez-Blasco et al., 2021; Zurita et al., 2016).

Although our knowledge of Pleistocene glyptodonts is being refined as a result of recent works, diagnostic elements to distinguish major clades are now unclear or poorly known. Although craniodental and skeletal characters are relatively well-represented in phylogenetic matrices for glyptodonts, morphological studies aiming at primary homology hypotheses among genera concern studies in only a few of them. For example, one of the most recent phylogenetic matrices at the evolutionary-scale of Pleistocene glyptodonts contains 20 craniodental characters of which only five show hypotheses of homologies among genera, i.e., less than 9% of the matrix (Núñez-Blasco et al., 2021). In addition, endocranial structures remain non-existent in the phylogenetic matrices to date, while several authors have emphasized

their potential relevance for the phylogeny of glyptodonts (e.g., Le Verger et al., 2021; Tambusso & Fariña, 2015a; Tambusso et al., 2021). However, the discovery of diagnostic elements to differentiate or group Pleistocene glyptodont ideally requires a sufficiently complete amount of remains for comparison.

The Pleistocene Pampean Region of Argentina is rich in fossiliferous beds, first explored by Charles Darwin and Alcide D'Orbigny around 1830 and later by many others (e.g., Ameghino, 1881, 1908; Cione & Tonni, 2005; Prado et al., 2021; Verzi et al., 2004). Among these fossil explorers is Santiago Roth, a Swiss-Argentinian palaeontologist who built up one of the largest collections from

expeditions to the Pampean Region and supplied several Swiss, Danish, and Argentinian museums with specimens (i.e., MCGL; MHNG; MLP; PIMUZ; ZMK—see Abbreviations) (Sánchez-Villagra et al., 2023; Voglino et al., 2023). Santiago Roth prospected over a large part of the region, an area of more than 600,000 km² (Fig. 1), during the late 19th and early 20th century. In accordance with the three stages that Ameghino (1881) grouped within the "Pampean formation", Santiago Roth defined the Inferior, Intermediate, and Superior Pampean, three units separated on the basis of their palaeontological content rather than their lithological differences (Ameghino, 1908). Nowadays, the Inferior Pampean unit comprises

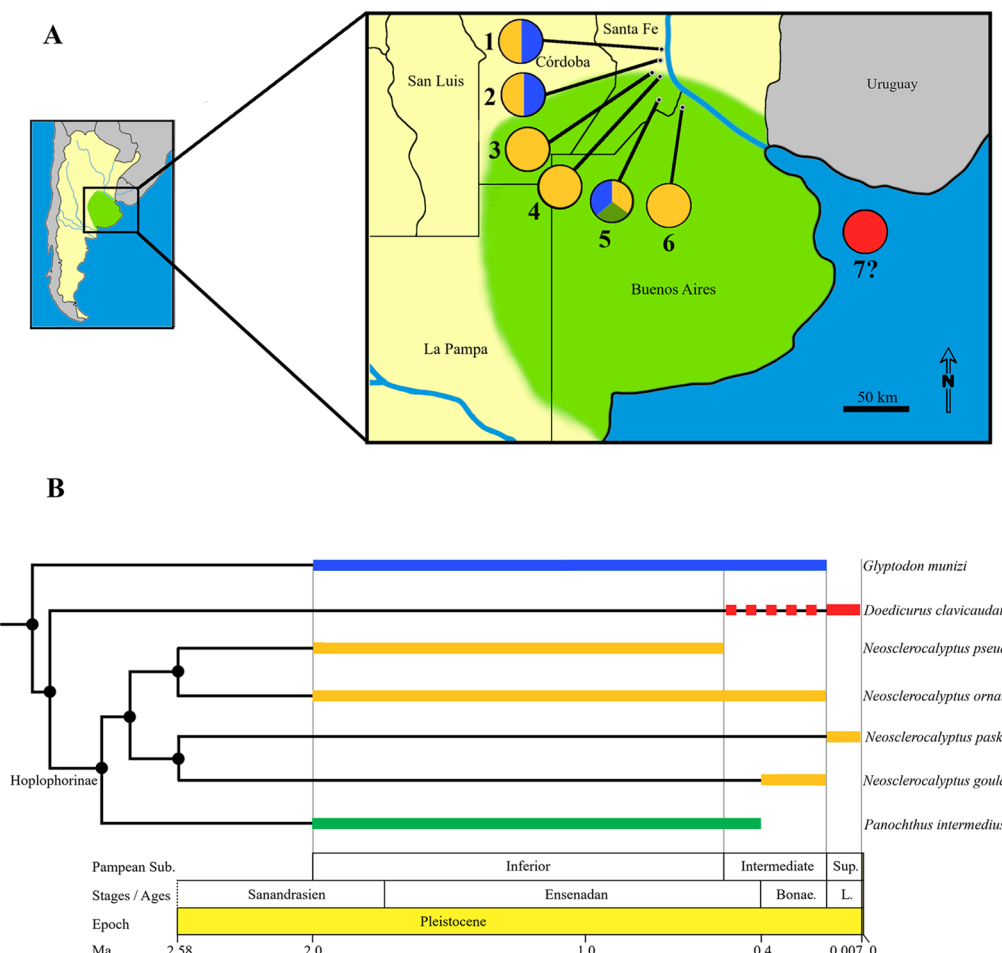


Fig. 1 Spatial, temporal, and phylogenetic context of the study. **A** Localities in the Pampean Region (green) of Argentina (yellow) according to Chichkoyan Kayayan (2017), Prado et al. (2021), and Voglino (2020). For each locality the proportion of each genus is indicated by the same color code as used in the tree. The numbered localities are: 1, San Lorenzo/Barranca San Lorenzo, Tonelero; 2, San Nicolás/Barranca San Nicolás, Tonelero; 3, Rosario/Barranca Rosario/Alverde près Rosario, Tonelero; 4, Arroyo de Cepeda; 5, Arroyo del Medio/Barranca del Arroyo del Medio; 6, Arroyo Pergamino; 7, Arroyo Pergo (locality lost or Arroyo Pergamino abbreviated). **B** Phylogeny of the studied glyptodonts following Nuñez-Blasco et al. (2021). The chronological scale is based on numerous works that have linked Roth's Pampean subdivisions with the stratigraphic Stages/Ages (see text). The nodes of the tree are not calibrated in time, but the stratigraphic extension of each species is indicated (see text for references). Bonae., Bonaerian; L, Lujanian; Sub, Subdivision; Sup, Superior

roughly the majority of the Ensenadan, the Intermediate Pampean unit corresponds to the late Ensenadan and the Bonaerian, and the Superior Pampean to the Lujanian (see Cione & Tonni, 1995; Cione et al., 2015; Hansen, 2019; Prado et al., 2021; Voglino, 2020; Voglino et al., 2023), thus covering a large part of the Pleistocene (see Geological Settings). Through the Pampean Region, Santiago Roth collected a large number of fossils belonging to the extinct South American mammals, especially megafauna, including several Rodentia, Carnivora, Perisodactyla, and Cetacea and other artiodactyls as well as emblematic clades, such as toxodonts, gomphotheres, and macrauchenias (Aguirre-Fernández et al., 2022; Roth, 1889). However, the most abundant representatives belong to xenarthrans, including ground sloths and glyptodonts. These comprise more than half of the collection housed in the PIMUZ (Le Verger, 2023). The Pampean Region, and thus the Santiago Roth Collection, is crucial for the study of glyptodonts, as the cranial remains present in the collection cover most of the major Pleistocene glyptodont genera (Fig. 1). Despite the high quality of the collection with regard to the diversity of Pleistocene glyptodonts, according to our knowledge, the specimens present in European institutions were rarely studied (Le Verger, 2023; Schulthess, 1920).

We conducted a comparative description of the cranial anatomy of Pleistocene glyptodonts present in the Santiago Roth Collections housed in Europe. Our study focused on the external cranial anatomy, including the mandible, and the endocranial traits of the inner ear, braincase, and related cranial canals. In addition to address the first comparative description of mostly unpublished specimens, our study allows us to highlight the general endocranial and external traits of the skull among the major South American genera of Pleistocene glyptodonts and to discuss their relevance for the systematics of this clade. We address issues of palaeoecology and diversity preceding extinction during the Pleistocene of the Pampean Region.

Materials and methods

Sampling

Specimens used in the present study are housed at the PIMUZ (Palaeontological collections of the Department of Paleontology, University of Zurich) and at the ZMK (Zoologisk Museum, København, Denmark, included in the Lausen Collection). We studied also glyptodonts housed at the MCGL (Musée Cantonal de Géologie Lausanne) and the MHNG (Museum d'Histoire Naturelle de Genève), but these were the same species as those stored at PIMUZ and ZMK, showed no significant intraspecific variation, and sometimes were much more fragmentary, thus, we do not report on them. Two almost complete

skulls (=cranium + mandible), four incomplete crania, and five incomplete mandibles were examined from the PIMUZ collection (Table 1). We also studied three almost complete skulls of *Glyptodon munizi*, *Neosclerocalyptus ornatus*, and *Panochthus intermedius* at the ZMK (Table 1), including remains of *Panochthus*, which is crucial to cover most of the glyptodont diversity present in the Pleistocene. The total number of specimens ($n=13$) from Roth collection corresponds to seven species of glyptodonts from the Pampean Region, including two unidentified glyptodonts at the specific level (Table 1—see Le Verger, 2023, for taxonomic assessment). Digital data for a major part of our specimens from the PIMUZ were acquired using X-ray micro-computed tomography (μ CT). Specimens were scanned at the Irchel Campus of the University of Zurich using Nikon XT H 225 ST. Three-dimensional reconstructions of the selected structures (see below) were performed using stacks of digital μ CT images with MIMICS v. 23.0 software (3D Medical Image Processing Software, Materialize, Leuven, Belgium). In addition, the three specimens from the ZMK were acquired by surface scanning using an Artec Spider. The visualization of 3D models was also conducted with AVIZO v. 8.0.0 software (Visualization Sciences Group, Burlington, MA, USA). All the specimens μ CT-scanned, or surface scanned will be available on MorphoMuseum for 3D models and on MorphoSource for μ CT-scans (see dedicated part in the present volume). The list of μ CT-scanned and surface-scanned specimens is specified in Table 1.

Virtual reconstruction of endocranial regions

Endocranial anatomy has only recently been explored in glyptodonts, in particular the braincase (Tambusso & Fariña, 2015a, 2015b; Tambusso et al., 2023), inner ear (Tambusso et al., 2021), and tooth alveoli and cranial canals (Le Verger et al., 2021). These investigations have revealed a systematic and functional signal for Cingulata (Billet et al., 2015a, 2015b; Coutier et al., 2017; Tambusso & Fariña, 2015a, 2015b; Tambusso et al., 2021, 2023). We reconstructed several endocranial elements of the neurocranium (Fig. 2) for three specimens: *Doedicurus clavicaudatus* (PIMUZ A/V 4148); *Glyptodon munizi* (PIMUZ A/V 461), and *Neosclerocalyptus pseudornatus* (PIMUZ A/V 439). We reconstructed the braincase while delineating the olfactory bulbs, cerebrum, and cerebellum in accordance with the work of Boscaini et al. (2020a) on *Catonyx taricensis* Gervais & Ameghino, 1880, an extinct ground sloth. All the canals connecting with the braincase were reconstructed and identified following Le Verger et al. (2021), which allowed us to make the link with the analysis of the external anatomy through the opening

Table 1 List of specimens from the Roth Collection housed at PIMUZ and ZMK and associated information

Specimen—reference	Institutional N°	Roth N°	Locality—age—anatomical part
<i>Glyptodon munizi</i> Ameghino, 1881	PIMUZ A/V 461*	283	Arroyo de Cepeda Late Ensenadan and the Bonaerian Complete skull bearing all teeth
<i>Glyptodon munizi</i> Ameghino, 1881	PIMUZ A/V 462/472*	79	San Lorenzo/Barranca San Lorenzo, Tonelero Late Sanandresian and a major part of the Ensenadan Subcomplete cranium bearing broken Mf1–Mf8
<i>Glyptodon munizi</i> Ameghino, 1881	PIMUZ A/V 463	135	Arroyo del Medio Late Ensenadan and the Bonaerian Subcomplete right Hemimandible bearing mf1–mf8
<i>Glyptodon munizi</i> Ameghino, 1881	ZMK 69/1885**	Hd 1–4	Arroyo del Medio Late Ensenadan and the Bonaerian Subcomplete skull bearing all teeth
<i>Glyptodon</i> sp. Owen, 1839b	PIMUZ A/V 4097	185	San Nicolás/Barranca San Nicolás, Tonelero Late Ensenadan and the Bonaerian Fragmented mandible bearing three molariforms
<i>Doedicurus clavicaudatus</i> Gervais & Ameghino, 1880	PIMUZ A/V 4148*	215	Arroyo Pergo (or Arroyo Pergamino abbreviated) Late Ensenadan and the Bonaerian Neurocranium and anteriormost part of the left zygomatic arch
<i>Neosclerocalyptus pseudornatus</i> Ameghino, 1889	PIMUZ A/V 439*	216	San Nicolás/Barranca San Nicolás, Tonelero Late Sanandresian and a major part of the Ensenadan Complete skull bearing all teeth
<i>Neosclerocalyptus ornatus</i> Owen, 1845	PIMUZ A/V 447*	226	San Lorenzo/Barranca San Lorenzo, Tonelero Late Sanandresian and a major part of the Ensenadan Incomplete cranium bearing Mf2–Mf8
<i>Neosclerocalyptus gouldi</i> Zurita, Carlini & Scillato-Yané, 2008	PIMUZ A/V 436/437*	278	Arroyo del Medio Late Ensenadan and the Bonaerian Incomplete neurocranium and mandible bearing mf1–mf7
<i>Neosclerocalyptus gouldi</i> Zurita, Carlini & Scillato-Yané, 2008	ZMK 77/1888**	161	Arroyo Pergamino Lujanian Subcomplete skull bearing all teeth
<i>Neosclerocalyptus paskoensis</i> Zurita, 2002	PIMUZ A/V 438	124	Rosario/Barranca Rosario/Alverde près Rosario, Tonelero Lujanian Incomplete right and left hemimandible
<i>Neosclerocalyptus</i> sp. Paula Couto, 1957	PIMUZ A/V 442*	182	Arroyo Pergamino Lujanian Incomplete hemimandible bearing 3 molariforms (young individual)
<i>Panochthus intermedius</i> Lydekker, 1895	ZMK 66/1885**	Hb1–4	Arroyo del Medio Late Ensenadan and the Bonaerian Subcomplete skull bearing all teeth

*, CT-scan available; **, Surface scan available

of the canals by the cranial foramina (Fig. 2). Finally, we also reconstructed the inner ears of the same three specimens, comparing the anatomy of the bony labyrinth among some glyptodonts. Besides the value for taxonomy and systematics, the studied endocranial structures provide information on functional and palaeoecological aspects, particularly with respect to cerebral evolution, vascularization and innervation, and locomotion (e.g., Coutier et al., 2017, Schade et al., 2022). In our sample, at least one representative of *Glyptodon* (PIMUZ A/V 461), *Doedicurus* (PIMUZ A/V 4148), and *Neosclerocalyptus* (PIMUZ A/V 439), exhibits all these three endocranial parts complete. Information on *Panochthus* is taken from the work of Tambusso

and Fariña (2015a) and Tambusso et al. (2021) on the species *Panochthus tuberculatus* Owen, 1845.

Measurements and estimations

To provide quantitative evaluation of our qualitative comparisons, we performed several measurements following numerous references regarding the cranial anatomy of glyptodonts (e.g., Núñez-Blasco et al., 2021; Tambusso & Fariña, 2015a) on the most complete specimens in our sample, plus several others (Fig. 2, Table 2). When specimens were incomplete, we produced estimates from complete specimens in the literature based on at least one comparable measurement. All measurements were made directly on the specimens using a Vernier Caliper with a

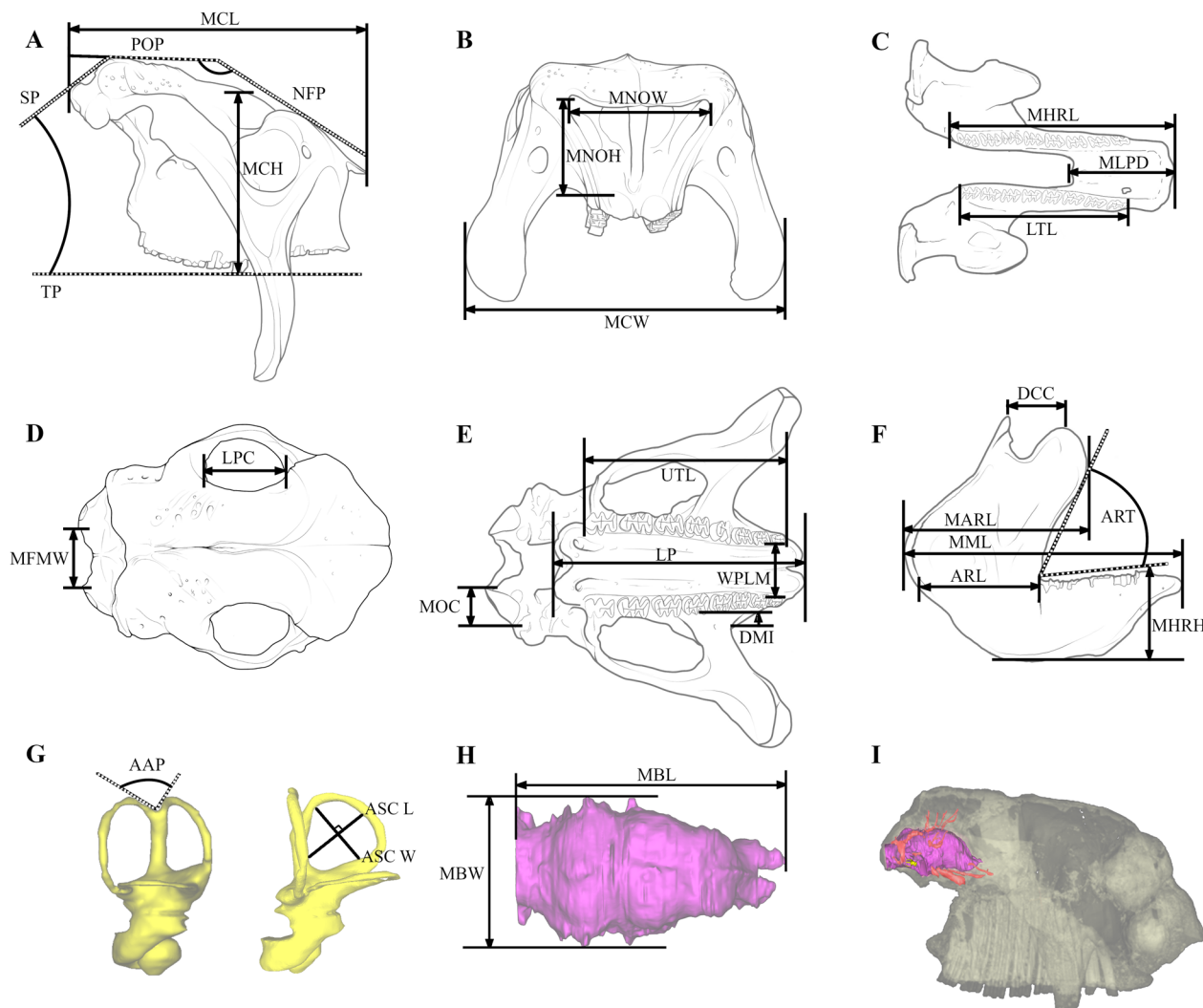


Fig. 2 Illustrations of the measurements defined in the present work on a skull of *Glyptodon munizi* (**A–F**; PIMUZ A/V 461) and selected endocranial structures on a cranium of *Neosclerocalyptus pseudornatus* (**G–I**; PIMUZ A/V 439). Cranium in lateral (**A**), anterior (**B**), dorsal (**D**), and ventral (**E**) views. Mandible in occlusal (**C**) and lateral (**F**) views. Endocranial structures are represented by an isolated and verticalized inner ear (**G**), an isolated braincase in dorsal view (**H**), and a cranium in transparency and in lateral view (**I**), showing the inner ear (yellow), braincase (pink), and associated neurocranial canals (red). See Table 2 for measurement definitions

precision of 0.05 mm and a Protractor. For the endocranial part, two linear measurements of the 3D braincase endocast, two linear and one new angular measurement of the inner ear (see Billet et al., 2012, 2015a, 2015b), the total raw volume of the 3D braincase endocast, and the relative volumes (i.e., divided by the total raw volume) of the olfactory bulbs, cerebrum, and cerebellum were obtained using MIMICS v. 23.0 software (Table 2).

Taxonomical considerations and phylogenetic framework

The first identifications referring to the glyptodonts collected by Santiago Roth were provided by him at the end of the 19th century (Roth, 1889). Subsequently,

Schulthess (1920) reviewed all the specimens in the PIMUZ Collection and made taxonomic corrections. Guth (1961) reassessed some specimens from this collection. Since then, no taxonomic update has been made except for a few isolated and unpublished notes. As the assessment of the diversity of glyptodonts has changed considerably (e.g., Fernicola, 2008; Fernicola & Porpino, 2012; Zamorano & Brandoni, 2013), a taxonomic revision for the glyptodonts in our study was necessary (Le Verger, 2023). All the specimens of our sample were thus reassigned in accordance with this deferred work. Regarding the specimens from the ZMK, the three specimens are particularly complete

Table 2 Measurements (in cm/cm3) illustrated in Fig. 2

Cranial Measurement—Estimation	<i>Glyptodon munizi</i> PIMUZ A/V 461	<i>Doedicurus clavicaudatus</i> PIMUZ A/V 4148	<i>Neosclerocalyptus pseudornatus</i> PIMUZ A/V 439	<i>Neosclerocalyptus ornatus</i> PIMUZ A/V 447	<i>Neosclerocalyptus gouldi</i> ZMK 77/1888	<i>Panochthus intermedius</i> ZMK 66/1885
Maximum Cranial Length (MCL)	31	38.0*	32.7	33.4	28.1	41.5
Maximum Cranial Width (MCW)	28.5	36.0*	19.0	22.0*	22.5	30.5
Maximum Cranial Height (at the level of Mf4) (MCH)	12	—	15.0	17.4	17.3	21.9
Maximum Narial Opening Width (MNOW)	12	—	18.0	17.2	14.6	9.2
Maximum Narial Opening Height (MNOH)	6	—	6.0	7.2	10.8	6.5
Length of the Postorbital Constriction in dorsal view (LPC)	6	—	5.0	7.0	8.3	9.2
Upper Toothrow Length (UTL)	20.5	—	17.0	18.2	18.5	22.5
Length of the Palate (LP)	23.5	—	20.5	21.0*	23*	30.6
Width of the Palate at the Level of Mf1 (WPLM)	5.5	—	3.6	3.9	4.0*	4.7
Maximum Foramen Magnum Width (MFMW)	4.5	3.8	2.8	7.2	3.4	5.5
Distance between labial side of Mf4 and Infraorbital foramina in ventral view (DMI)	3.3	—	2.0	—	1.9	3.6
Maximum Occipital Condyles width (MOC)	3.2	3.9	2.4	3.0	2.3	2.9
Angle between the Supraoccipital Plane (SP) and the toothrow plane (TP)	40°	—	55°	45°	60°	50°
Angle between the Naso-Frontal Plane (NFP) and the Parieto-Occipital Plane (POP)	170°	—	180°	170°	155°	145°
Endocranial Measurement—Estimation	PIMUZ A/V 461	PIMUZ A/V 4148	PIMUZ A/V 439	—	—	—
Maximum Braincase endocast anteroposterior Length (MBL)	10.4	12.8	10.0	—	—	—
Maximum Braincase endocast mediolateral Width (MBW)	8.1	8.5	5.4	—	—	—
Braincase endocast volume (excluding canals)	236.6	255.7	99.0	—	—	—
Relative olfactory bulb volume	6.0%	8.0%	2.0%	—	—	—
Relative cerebrum volume	77.0%	80.0%	81.0%	—	—	—

Table 2 (continued)

Endocranial Measurement—Estimation	PIMUZ A/V 461	PIMUZ A/V 4148	PIMUZ A/V 439	-	-	-
Relative cerebellum volume	17.0%	12.0%	17.0%	-	-	-
Angle between Anterior semicircular canal and Posterior semicircular canal (AAP)	69°	102°	104°	-	-	-
Length diameter of the Anterior Semicircular Canal (ASC L)	6.6	9.3	7.1			
Width diameter of the Anterior Semicircular Canal (ASC W)	6.4	7.9	7.0			
Length diameter of the Posterior Semicircular Canal (PSC L)	7.8	8.7	7			
Width diameter of the Posterior Semicircular Canal (PSC W)	7.9	8.3	6.1			
Length diameter of the Lateral Semicircular Canal (LSC L)	6.6	5.6	7.5			
Width diameter of the Lateral Semicircular Canal (LSC W)	7.3	6.8	7.8			
Mandibular Measurement—Estimation	PIMUZ A/V 461	-	PIMUZ A/V 439	PIMUZ A/V 437	ZMK 77/1888	ZMK 66/1885
Maximum Mandibular Length (MML)	31.5	-	26.3	-	27.3	35.4
Maximum Horizontal Ramus Length (MHRL)	26.5	-	16.5	21.0*	21	30.2
Maximum Horizontal Ramus Height (MHRH)	7.0	-	5.2	5.1	7.8	9.7
Lower Toothrow Length (LTL)	19.5	-	14.0	19.0*	19.8	21
Ascending Ramus Length at the level of the most posterior point of the mf6 (ARL)	14.0	-	18.5	11.0*	10.8	14.5
Maximum Ascending Ramus Length (MARL)	24.3	-	4.6	-	10.8	15.4
Maximum Length of the Pre-Dentary area (MLPD)	5.0	-	-	-	12	16
Distance between the most dorsal point of the Coronoid and the Condylar processes (DCC)	3.2	-	-	-	4.9	8.2
Angle between the ascending Ramus plane and the lower Toothrow plane (ART)	70°	-	85°	90°	85°	65°

*, estimated measurement

and have been taxonomically reassigned following Le Verger (2023).

Because of the recent inclusion of glyptodonts within armadillos brought by both morphological and molecular phylogenetic studies (Delsuc et al., 2016; Gaudin & Wible, 2006; Mitchell et al., 2016), the taxonomic status of glyptodonts at a higher rank than genus is still subject to debate (see the discussion of Delsuc et al., 2016, and Gaudin & Lyon, 2017). As the present study does not aim to resolve this issue, we have opted for a comparison at the generic level, where the monophyly of the groups is not debated. Regarding the phylogenetic context for glyptodonts, the literature is rich with studies that have addressed various questions about the evolutionary history of the clade. Some works address more broadly the position of glyptodonts within the Cingulata (e.g., Billet et al., 2011; Gaudin & Wible, 2006). Other studies have focused more specifically on the overall evolutionary history of the clade (e.g., Fernicola, 2008; Fernicola et al., 2018; Porpino et al., 2010) or on its diversity over a given period, such as the Pleistocene (Cuadrelli et al., 2020; Nuñez-Blasco et al., 2021; Zurita et al., 2013, 2014). Finally, some works focus more specifically on a clade within the glyptodonts (e.g., Zamorano & Brandoni, 2013; Zurita et al., 2017). In the present study, our interest is in a diversity of glyptodonts known only during the Pleistocene. Accordingly, here, the phylogeny used to discuss the anatomical traits (Fig. 1) is derived from Nuñez-Blasco et al., (2021) and corresponds to the most parsimonious tree resulting from a cladistic analysis based on a widely used and reworked matrix of glyptodonts (Cuadrelli et al., 2020; Fernicola, 2008; Porpino et al., 2010; Zamorano & Brandoni, 2013; Zurita et al., 2013, 2014, 2017). The updated matrix consists of 23 taxa and 57 characters of which 20 characters are from the skull (including teeth and mandibles) and includes all the species in our study except for *Neosclerocalyptus gouldi* and *Neosclerocalyptus pseudornatus*, which we added to the tree topology based on Zurita et al., (2013). Our purpose here is not to perform a new phylogenetic analysis but to have a phylogenetic framework to discuss the anatomical traits from our comparative analysis focused at the genus level. The homological hypotheses discussed based on this phylogenetic framework are also discussed in relation to one of the most recent alternative phylogenetic hypotheses of relationships among glyptodonts (see Fernicola et al., 2018).

Approach for comparative anatomy

We focused our investigation on the external anatomy of the cranium and mandible, and then on the endocranial parts of the neurocranium. Only informative comparisons (i.e., at least two genera share a common anatomical

trait independently of the other genera) are presented in results and discussed. Dental homology for glyptodonts is unresolved and we follow conventional nomenclature considering the entire set of teeth as molariforms (e.g., González Ruiz et al., 2015). For external cranial anatomy and in addition of many description for glyptodont genera or subfamilies (e.g., Cuadrelli et al., 2020; Nuñez-Blasco et al., 2021; Zamorano et al., 2021; Zurita et al., 2011b), we followed mainly Wible and Gaudin (2004) on *Euphractus sexcinctus* Linnaeus, 1758, complemented with the detailed anatomical description of the pampatheres *Holmesina floridanus* Robertson, 1976 (Gaudin & Lyon, 2017), a representative of the glyptodont's sister-group (Billet et al., 2011; Gaudin & Wible, 2006). For anatomical nomenclature associated with the 3D braincase endocast, we cross-referenced different nomenclatures (Butler & Hodos, 1996; Dechaseaux, 1958, 1962; Dozo, 1998; Gervais, 1869). For cranial canals, we followed the nomenclature used by Le Verger et al. (2021). For inner ear anatomy we used the same protocol as Billet et al. (2015b). However, for *Doedicurus clavicaudatus*, we complemented our approach with the literature associated with the anatomy of Doedicurinae (e.g., Lydekker, 1894; Nuñez-Blasco et al., 2021; Zurita et al., 2016), and for the internal anatomy of *Panochthus*, we compared our specimen with the illustrated braincase and inner ear from Tambusso and Fariña (2015a) and Tambusso et al., (2021, see also Tambusso et al., 2023).

Geological Setting

The "Pampean Formation" was initially defined by the surface sediments covering the Pampean Region (Bravard, 1857; Darwin, 1845; D'Orbigny, 1842). Then, Florentino Ameghino created three subdivisions for the "Pampean Formation" in accordance with the lithological homogeneity that he proposed to refine with the help of the fossil record (Ameghino, 1881, 1908). As mentioned by Prado et al. (2021), since then many works tried to clarify the boundaries of these three subdivisions (Cione & Tonni, 1995, 1996; Cione et al., 1999; Deschamps & Tomassini, 2016; Pardiñas & Deschamps, 1996; Soibelzon et al., 2009, 2019; Tonni et al., 1992; Verzi & Lezcano, 1996; Verzi et al., 2004). For the present study, we refer to the work of Prado et al. (2021), which updated the state of the art of the Pampean Region, and considering the work of Chichkoyan Kayayan (2017), we specify the geographical position of the localities concerned by our sampling in Fig. 1 (see also Voglino et al., 2023). The three units defined by Santiago Roth as the Inferior, Intermediate, and Superior Pampean refer to the Ensenada and Buenos Aires formations of the Pampean Region (Navel et al., 2000; Riggi et al., 1986; Tonni et al., 1999). The former two belong to the Ensenadan stage covering the Early and

Middle Pleistocene (~1.95–1.77–0.4 Mya), while the latter covers the Bonarian and Lujanian stages belonging to the Late Pleistocene (0.4–~0.007 Mya). Consequently, the "Pampean Formation" extends over a large part of the Pleistocene (see Voglino et al., 2023).

Institutional abbreviations

MCGL, Musée Cantonal de Géologie Lausanne, Switzerland; MHNG, Museum d'Histoire Naturelle de Genève, Switzerland; MLP, Museo de la Plata, Buenos Aires, Argentina; PIMUZ, Palaeontological Institute and Museum of the University of Zurich, Switzerland; ZMK, Zoologisk Museum, København, Denmark.

Other abbreviations

K, character; mf, lower molariform; Mf, upper molariform, µCT, X-ray micro-computed tomography.

Systematic Palaeontology

Xenartha Cope, 1889

Cingulata Illiger, 1811

Glyptodontoidea Gray, 1869

Glyptodontidae Gray, 1869

External anatomical comparisons

Concerning the completeness, *Glyptodon munizi* (PIMUZ A/V 461 and ZMK 69/1885), *Neosclerocalyptus pseudornatus* (PIMUZ A/V 439), *Neosclerocalyptus gouldi* (ZMK 77/1888), as well as *Panochthus intermedius* (ZMK 66/1885) are the specimens with the best preservation. The whole crania of *Glyptodon munizi* (PIMUZ A/V 462) and *Neosclerocalyptus ornatus* (PIMUZ A/V 447) present a relatively large missing portion, mostly the zygomatic arches and the basicranium. Both of them are crushed, resulting in almost no visibility of the cranial sutures. For *Doedicurus clavicaudatus* (PIMUZ A/V 4148), only the neurocranium and anterior part of the left zygomatic arch including the maxillary with three Mf are preserved.

Anterior view

The cranium of *Glyptodon munizi* (PIMUZ A/V 461 and ZMK 69/1885) and *Doedicurus clavicaudatus* (Núñez-Blasco et al., 2021) are subrectangular (Fig. 3), in contrast to *Neosclerocalyptus* species (PIMUZ A/V 439; PIMUZ A/V 447; ZMK 77/1888) and *Panochthus intermedius* (ZMK 66/1885) for which the overall shape of the cranium in anterior view is rounded (Fig. 3; Zamorano et al., 2014a; Zurita et al., 2011b). This distinction is particularly emphasized by the cranial roof and its contact with the posterior part of the zygomatic arches in this view. The latter is not preserved for our specimens, but the zygomatic arches show a large range of

variation within Pleistocene glyptodonts (comparable by illustrated specimens—e.g., Fernicola & Porpino, 2012; Zurita et al., 2011b; Zurita et al., 2013). The overall shape of the cranium is also influenced by the shape of the descending processes of the zygomatic arch. In this view, in most glyptodonts, the descending processes of the zygomatic arch exhibit a medial concave curvature towards the process tip (Núñez-Blasco et al., 2021; Zamorano et al., 2014a). In *Glyptodon munizi* (PIMUZ A/V 461 and ZMK 69/1885), *Neosclerocalyptus pseudornatus* (PIMUZ A/V 439), and *Neosclerocalyptus gouldi* (ZMK 77/1888), this curvature is less pronounced, being practically straight dorsoventrally (Fig. 3). *Doedicurus clavicaudatus* (Núñez-Blasco et al., 2021), *Panochthus intermedius* (ZMK 66/1885), *Neosclerocalyptus gouldi* (ZMK 77/1888), and *Neosclerocalyptus pseudornatus* (PIMUZ A/V 439) share a proportionally similar transverse width of the descending process of the zygomatic arch whereas, in *Glyptodon munizi* (PIMUZ A/V 461 and ZMK 69/1885), the descending process of the zygomatic arch is wider and more dorsoventrally elongated than in the other glyptodonts. Among the species of *Neosclerocalyptus*, the infraorbital foramen, transmitting the infraorbital vein, artery, and nerve for the vascularization and the innervation of the snout, is elliptical (Zurita, 2007), with *Neosclerocalyptus ornatus* exhibiting the greatest width within the genus (Zurita et al., 2008). *Neosclerocalyptus pseudornatus* (PIMUZ A/V 439) is the only species of the sample where the infraorbital foramen is directed ventroanteriorly instead of anteroventrally. The infraorbital foramen in Doedicurinae (Núñez-Blasco et al., 2021), *Panochthus intermedius* (ZMK 66/1885), and *Glyptodon munizi* (PIMUZ A/V 461 and ZMK 69/1885) are subcircular. In the latter, the infraorbital foramen expands to a ventral groove, which is not visible in *Doedicurus clavicaudatus* (Cuadrelli et al., 2019; Núñez-Blasco et al., 2021; Zurita et al., 2013). In the smallest glyptodonts (Fariña et al., 1998; Vizcaíno et al., 2011), *Neosclerocalyptus pseudornatus* (PIMUZ A/V 439), *Neosclerocalyptus ornatus* (PIMUZ A/V 447), and *Neosclerocalyptus gouldi* (ZMK 77/1888), the orbit is hidden by the ossified nasal cartilage, an unique feature among vertebrates (Fernicola et al., 2012). The orbit exhibits a completely lateral orientation, whereas in larger size species (Fariña et al., 1998; Vizcaíno et al., 2011), as in *Glyptodon munizi* (PIMUZ A/V 461 and ZMK 69/1885) and *Panochthus intermedius* (ZMK 66/1885), the orbit is visible in anterior view with a more lateral position leading to a more convergent orbit orientation than in *Neosclerocalyptus* species (Zamorano et al., 2014a). This trend is confirmed in the largest representative, *Doedicurus clavicaudatus* (Núñez-Blasco et al., 2021). More anteriorly, all glyptodonts exhibit two large narial openings separated on the midline by

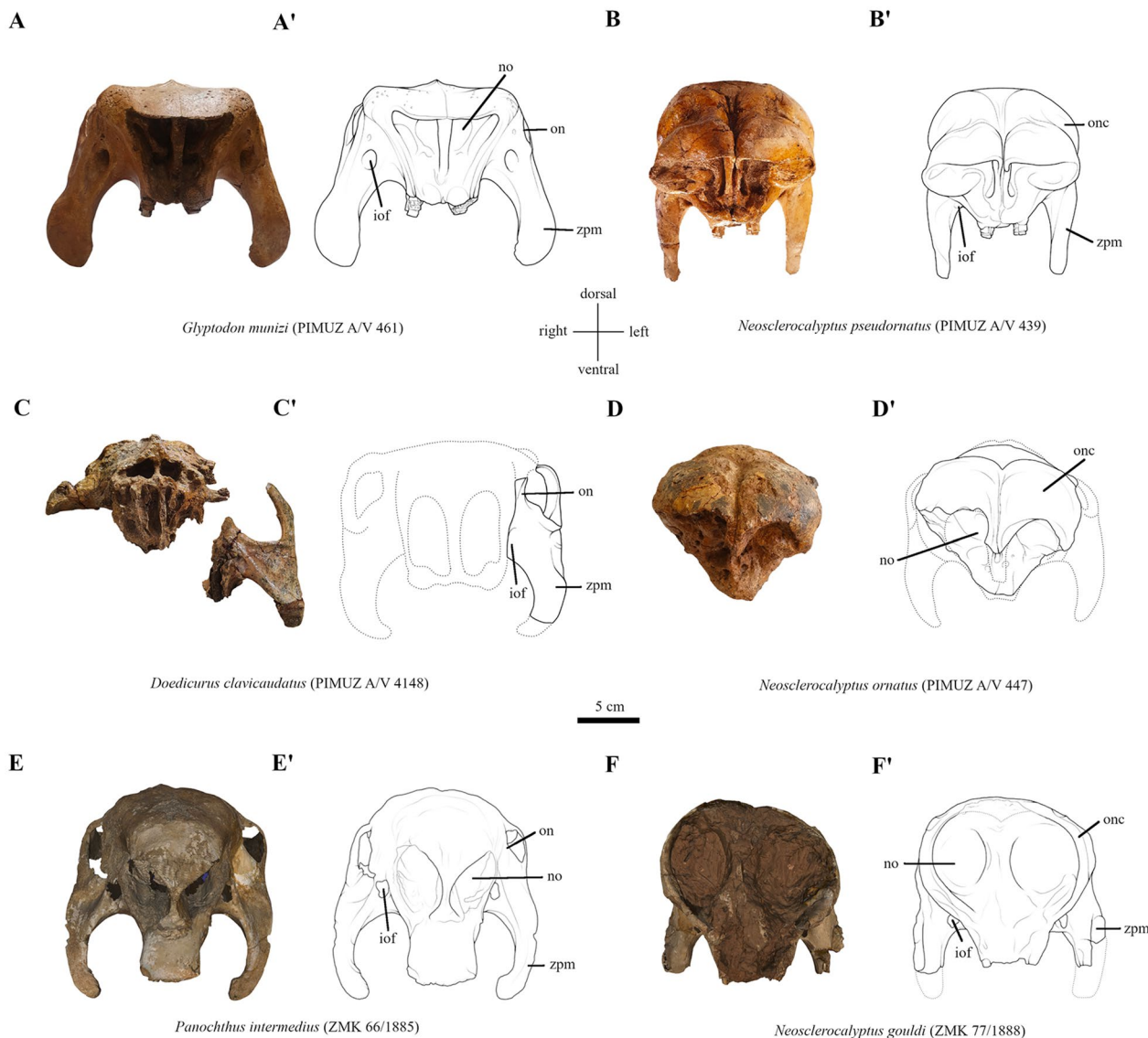


Fig. 3 Plate of the most complete studied crania in anterior view and their associated schematic drawings housed at PIMUZ and ZMK of Pleistocene glyptodonts of the Pampean Region collected by Santiago Roth. iof, infraorbital foramen; no, narial opening; on, orbital notch; onc, ossified nasal cartilage; zpm, descending process of the zygomatic arch

a septomaxilla. In *Glyptodon munizi* (PIMUZ A/V 461 and ZMK 69/1885), the narial opening is subtriangular, with strongly pronounced narial notches, whereas in *Doedicurus clavicaudatus* (Núñez-Blasco et al., 2021), the shape of this opening is rectangular and dorsoventrally elongated. All other species show a different narial opening. In *Panochthus intermedius* (ZMK 66/1885), and other species of the genus, most of the narial openings are covered by the subtriangular descending nasal bone resulting in pronounced narial notches (Zamorano et al., 2014a). Among the *Neosclerocalyptus* species, the shape of the narial openings differ according to shape of the

ossified nasal cartilage. They range from a very reduced shape open ventrally as in *Neosclerocalyptus pseudornatus* (PIMUZ A/V 439) to a very large shape with two circular openings as in *Neosclerocalyptus gouldi* (PIMUZ A/V 447; Fig. 3) or *Neosclerocalyptus paskoensis* (Zurita et al., 2011b).

Dorsal view

In its general appearance, the cranium is rectangular with a length greater than the width for all glyptodonts (Table 2; for Doedicurinae see Núñez-Blasco et al., 2021); however, the incompleteness of the material does not

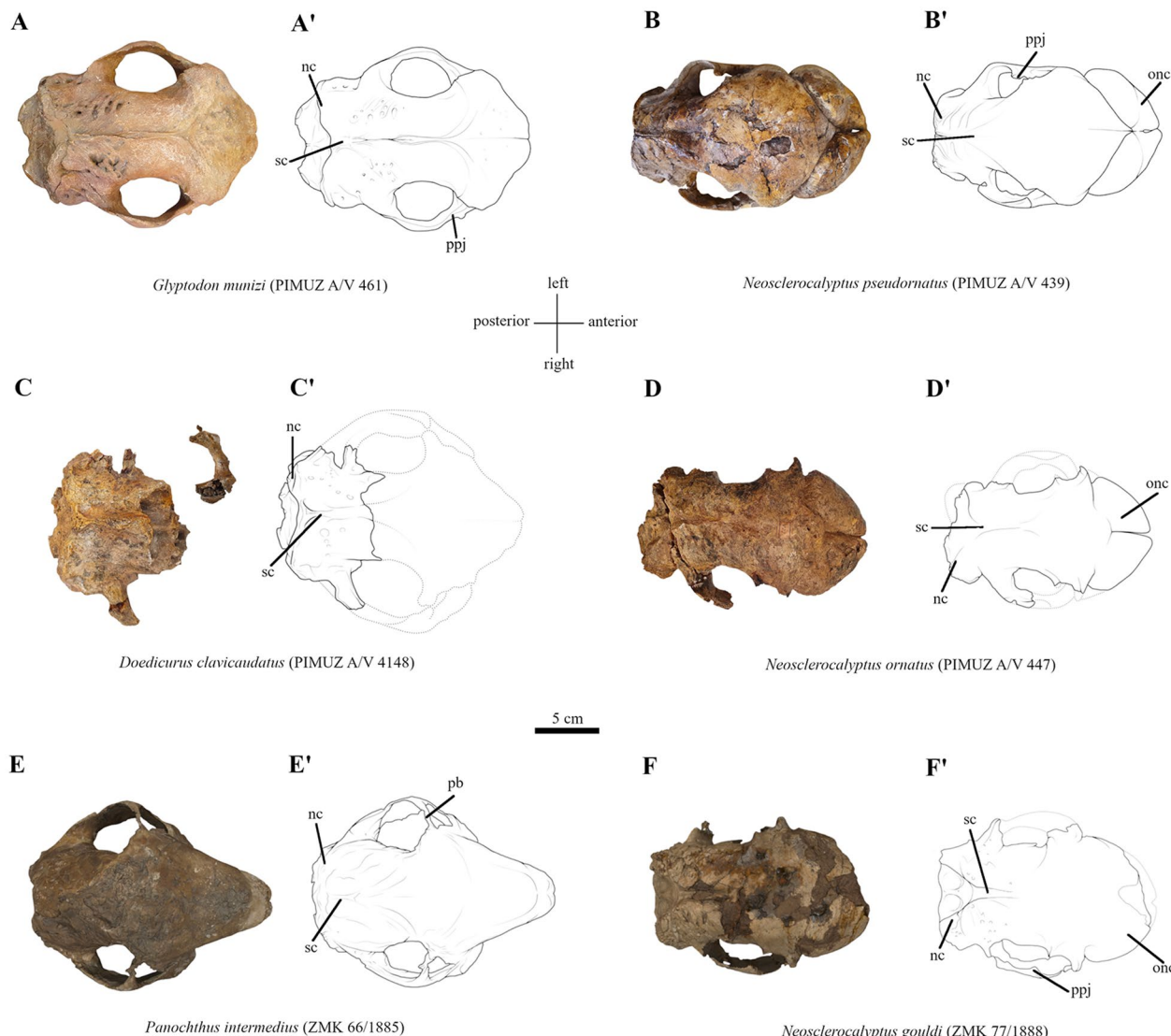


Fig. 4 Plate of the most complete studied crania in dorsal view and their associated schematic drawings housed at PIMUZ and ZMK of Pleistocene glyptodonts of the Pampean Region collected by Santiago Roth. nc, nuchal crest; onc, ossified nasal cartilage; pb, postorbital bar; ppj, postorbital process of jugal; sc, sagittal crest

allow a strict comparison of these cranial dimensions (Fig. 4). The main difference in our sample is the presence of ossified nasal cartilage in the three *Neosclerocalyptus* species compared to other glyptodonts. *Neosclerocalyptus pseudornatus* (PIMUZ A/V 439) shows two nasal bullae on each side of the cranium and a relatively more posterior position of the orbit than in *Neosclerocalyptus ornatus* (PIMUZ A/V 447) and *Neosclerocalyptus gouldi* (ZMK 77/1888; Fig. 4). Regardless of this feature, *Neosclerocalyptus pseudornatus* (PIMUZ A/V 439) exhibits a kite-like shape resulting from a nasal bone pointing anteriorly in a V-shape and a greater width at the level of the orbit than at the level of the zygomatic arches

posterior margin. This general shape implies a reduced parieto-occipital area compared to the naso-frontal area in the dorsal view. In *Neosclerocalyptus ornatus* (PIMUZ A/V 447), *Neosclerocalyptus gouldi* (ZMK 77/1888), and *Glyptodon munizi* (PIMUZ A/V 461 and ZMK 69/1885), this reduction in width in the posterior part is not as pronounced, leading to an overall shape more comparable to an hourglass, although the postorbital constriction is more marked in *Neosclerocalyptus pseudornatus* (PIMUZ A/V 439). *Doedicurus clavicaudatus* (PIMUZ A/V 4148) cannot be compared to the other specimens with respect to the anterior part of the cranium, but it exhibits a laterally flattened neurocranium, suggesting

that this species does not show a reduction of the parieto-occipital region as in *Neosclerocalyptus pseudornatus* (PIMUZ A/V 439). *Doedicurus clavicaudatus* (PIMUZ A/V 4148) also exhibits a more prominent sagittal crest than other glyptodonts. Anteriorly, the sagittal crest forms the temporal line in other specimens (for *Doedicurinae* see Nuñez-Blasco et al., 2021), not preserved in *Doedicurus clavicaudatus* (PIMUZ A/V 4148). In *Glyptodon munizi* (PIMUZ A/V 461 and ZMK 69/1885), the temporal line bifurcates at the level of Mf6, whereas in *Neosclerocalyptus* species the temporal line bifurcates at the level of the temporal fossa's posterior margin (i.e., at the level between Mf7 and Mf8; Fig. 4). Unlike *Neosclerocalyptus* species and *Glyptodon munizi* (PIMUZ A/V 461 and ZMK 69/1885), *Doedicurus clavicaudatus* (PIMUZ A/V 4148) shows a stronger transverse protrusion of the most posterior part of the zygomatic process of the squamosal, a feature also observable in *Panochthus intermedius* (ZMK 66/1885). In this same zygomatic arch protrusion, the curvature formed by the zygomatic arch in its most posterior portion is well-pronounced in *Neosclerocalyptus pseudornatus* (PIMUZ A/V 439), in contrast to other glyptodonts. This steeper trajectory of the zygomatic arch is coupled with a general reduction of the relative proportion of the temporal fossa in *Neosclerocalyptus pseudornatus* (PIMUZ A/V 439) while in all other glyptodonts, the temporal fossa is wider. The relative reduction of the temporal fossa is also related to the presence of an incomplete postorbital bar in *Neosclerocalyptus pseudornatus* (PIMUZ A/V 439) and *Neosclerocalyptus gouldi* (ZMK 77/1888) by the combination of a postorbital process and a frontal process of the jugal, both of which are strongly pronounced. The postorbital process is also present in *Glyptodon* but without a visible process emerging from the jugal (Fig. 4). In *Panochthus intermedius* (ZMK 66/1885), and in *Doedicurus clavicaudatus* (Nuñez-Blasco et al., 2021), the postorbital process is fully fused as a postorbital bar (Fig. 4). Regarding the cranial roof, there is no major difference within glyptodonts, the parietal is less than half as short as the frontal and has a variable number of foramina for the *rami temporales* (see also Nuñez-Blasco et al., 2021; Zamorano et al., 2014a). The occiput inclination, however, is stronger in *Glyptodon munizi* (PIMUZ A/V 461 and ZMK 69/1885), a species for which the occipital condyles exhibit a more lateral position and anterolateral orientation than in *Doedicurus clavicaudatus* (PIMUZ A/V 4148) and *Panochthus intermedius* (ZMK 66/1885). The latter two show relatively similar nuchal crests, with an anteriorly positioned occipital protuberance compared to *Glyptodon munizi* (PIMUZ A/V 461 and ZMK 69/1885) and *Neosclerocalyptus* species, except

for *Neosclerocalyptus ornatus* (PIMUZ A/V 447; Fig. 4; see also Zurita et al., 2011b).

Lateral view

The anteroventral inclination of the naso-frontal area in relation to the parieto-occipital region is a highly variable feature among glyptodonts, with an angle of about 150° in *Panochthus intermedius* (ZMK 66/1885) and about 160°–170° in *Glyptodon munizi* (PIMUZ A/V 461 and ZMK 69/1885), 170° in *Neosclerocalyptus ornatus* (PIMUZ A/V 447) and *Neosclerocalyptus gouldi* (ZMK 77/1888) and up to 180° in *Neosclerocalyptus pseudornatus* (PIMUZ A/V 439), without the consideration of the ossified nasal cartilage (Fig. 5). While *Neosclerocalyptus* species show a reduced inclined nasal, in *Panochthus intermedius* (ZMK 66/1885), the nasal is elongated and strongly anteroventrally inclined. *Glyptodon munizi* (PIMUZ A/V 461 and ZMK 69/1885) shows the same anteroposterior inclination of the nasal, but with a less prominent elongation of the frontal. In *Neosclerocalyptus pseudornatus* (PIMUZ A/V 439), the unique well-developed ossified nasal cartilages exhibit an anteroposteriorly inclined point-like structure at the anterior tip. The diverse forms of the ossified nasal cartilages of *Neosclerocalyptus* species are inclined anteroventrally, forming an angle of about 150° with the naso-frontal area in *Neosclerocalyptus pseudornatus* (PIMUZ A/V 439), contrary to the inclination of *Neosclerocalyptus ornatus* (PIMUZ A/V 447) and *Neosclerocalyptus gouldi* (ZMK 77/1888) of about 160° due to the higher pneumatization of the paranasal sinuses (Zurita et al., 2011b). Regarding the posterior inclination of the parieto-occipital region of the cranium in relation to the upper toothrow, in *Glyptodon munizi* (PIMUZ A/V 461 and ZMK 69/1885) and *Doedicurus clavicaudatus* (PIMUZ A/V 4148), the area is inclined upwards, differing from the subparallel course of the parieto-occipital area observed in *Neosclerocalyptus pseudornatus* (PIMUZ A/V 439) and the downwards inclination of the parieto-occipital region of *Panochthus intermedius* (ZMK 66/1885), *Neosclerocalyptus gouldi* (ZMK 77/1888), and *Neosclerocalyptus ornatus* (PIMUZ A/V 447). This inclination of the parieto-occipital area results in a general convex shape of the cranial roof in the latter three species and in different positions of the basicranium with respect to the dorsal margin of the orbit among the different genera. The basicranium has a more dorsal position relatively to the toothrow in *Glyptodon munizi* (PIMUZ A/V 461 and ZMK 69/1885) and *Doedicurus clavicaudatus* (PIMUZ A/V 4148) in contrast to *Neosclerocalyptus* species, where the basicranium lies below the horizontal level of the dorsal margin of the orbit (Fig. 5). An intermediate position of the basicranium can be found in *Panochthus intermedius*

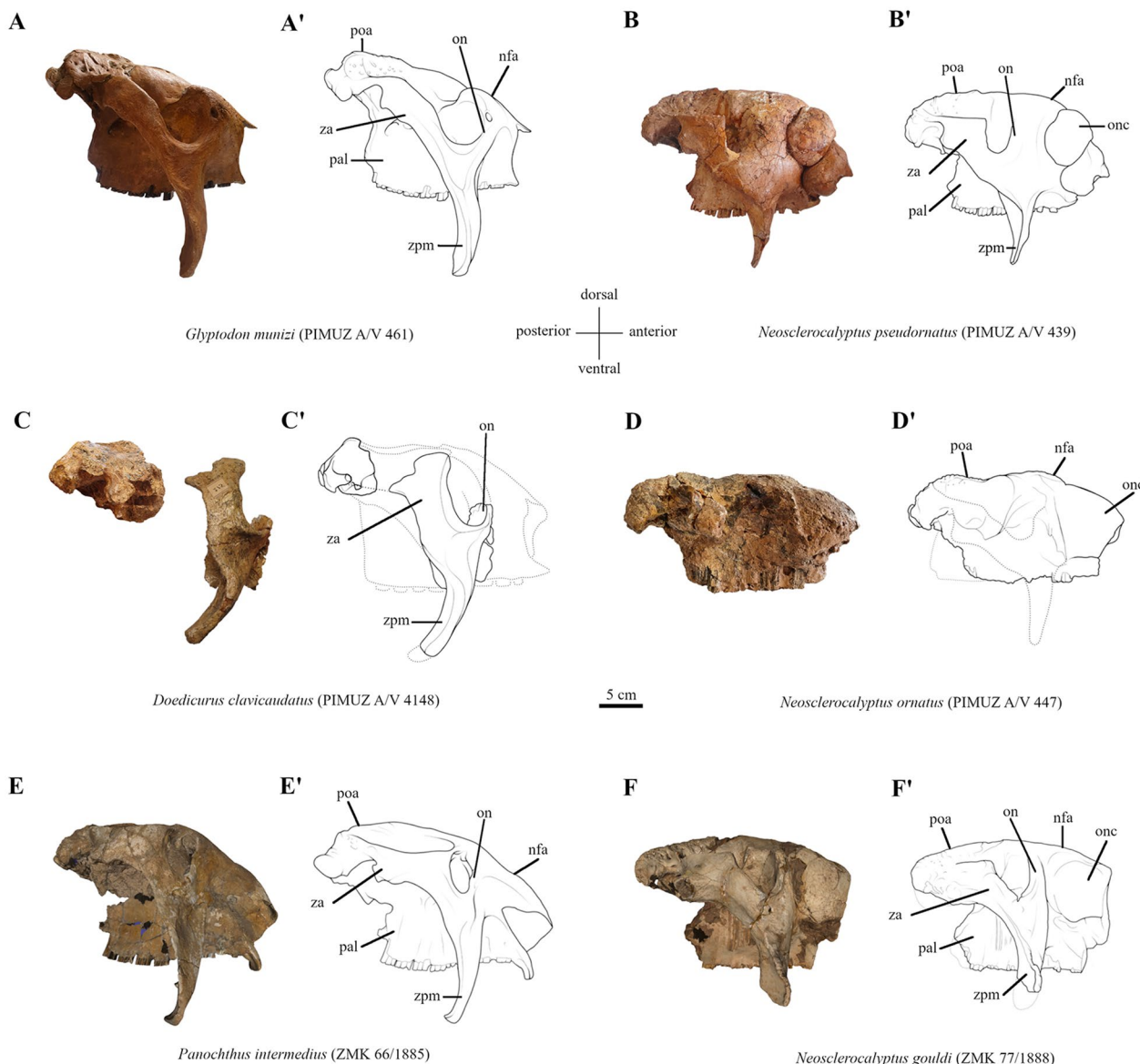


Fig. 5 Plate of the most complete studied crania in lateral view and their associated schematic drawings housed at PIMUZ and ZMK of Pleistocene glyptodonts of the Pampean Region collected by Santiago Roth. nfa, nasal-frontal area; on, orbital notch; onc, ossified nasal cartilage; pal, palatine; poa, parietal-occipital area; za, zygomatic arch; zpm, descending process of the zygomatic arch

(ZMK 66/1885). Consequently, the palate is dorsoventrally elongated in *Doedicurus clavicaudatus* (PIMUZ A/V 4148) and *Glyptodon munizi* (PIMUZ A/V 461 and ZMK 69/1885). Subsequently, the zygomatic process of the squamosal inclines in an anteroventral direction in *Glyptodon munizi* (PIMUZ A/V 461 and ZMK 69/1885), *Panochthus intermedius* (ZMK 66/1885), and *Doedicurus clavicaudatus* (Núñez-Blasco et al., 2021), whereas *Neosclerocalyptus gouldi* (ZMK 77/1888) and *Neosclerocalyptus pseudornatus* (PIMUZ A/V 439) exhibit a more horizontal course of the zygomatic process of the

squamosal. The zygomatic arch is high and more dorsally elongated in the latter two species, in contrast to the remaining species in which the zygomatic process of the squamosal is thinner dorsoventrally and more anteroposteriorly elongated. The orbit has a middle position in the length of the cranium in *Neosclerocalyptus* species and *Panochthus intermedius* (ZMK 66/1885). In *Doedicurus clavicaudatus* (Núñez-Blasco et al., 2021) and *Glyptodon munizi* (PIMUZ A/V 461 and ZMK 69/1885) the orbit has a more anterior position than in *Neosclerocalyptus* and *Panochthus*; *Neosclerocalyptus* species

exhibiting the smallest and most posteriorly situated orbit. The orbits in *Doedicurus clavicaudatus* (Núñez-Blasco et al., 2021) and *Neosclerocalyptus* species (see also Zurita et al., 2008) are subelliptical and dorsoventrally enlarged compared to the more circular orbit of *Glyptodon munizi* (PIMUZ A/V 461 and ZMK 69/1885) and *Panochthus intermedius* (ZMK 66/1885; Fig. 5). The well-developed postorbital process is situated at the level of the contact between Mf4 and Mf5 in *Neosclerocalyptus pseudornatus* (PIMUZ A/V 439) and *Glyptodon munizi* (PIMUZ A/V 461 and ZMK 69/1885), differing from *Neosclerocalyptus gouldi* (ZMK 77/1888) and *Panochthus intermedius* (ZMK 66/1885), for which the postorbital process starts at the level of the Mf5. In lateral view, *Glyptodon munizi* (PIMUZ A/V 461 and ZMK 69/1885) as well as *Neosclerocalyptus gouldi* (ZMK 77/1888) show a more pronounced posterior inflection of the descending process of the zygomatic arch. In all genera, the supraoccipital is inclined anterodorsally, with *Neosclerocalyptus pseudornatus* (PIMUZ A/V 439) exhibiting an angle of approximately 135° relative to the tooth row, 140° in *Neosclerocalyptus ornatus* (PIMUZ A/V 447), 145° in *Doedicurus clavicaudatus* (PIMUZ A/V 4148) and *Panochthus intermedius* (ZMK 66/1885), and the slightest inclination of 150° in *Glyptodon munizi* (PIMUZ A/V 461) (Table 2). The occlusal trajectory of the upper toothrow in all species except for *Neosclerocalyptus ornatus* (PIMUZ A/V 447) is sinusoidal in lateral view, where the posterior end of the toothrow is more ventrally situated than the anterior end. In contrast, *Neosclerocalyptus ornatus* (PIMUZ A/V 447) exhibits a horizontal course of the toothrow. Finally, in *Doedicurus clavicaudatus* (Núñez-Blasco et al., 2021), *Glyptodon munizi* (PIMUZ A/V 461 and ZMK 69/1885), and especially in *Panochthus intermedius* (ZMK 66/1885), the premaxillary is more prominent and anteroventrally inclined (Fig. 5).

Ventral view

Concerning the anterior maxillary/premaxillary area, *Neosclerocalyptus gouldi* (ZMK 77/1888), *Neosclerocalyptus ornatus* (PIMUZ A/V 447), *Neosclerocalyptus pseudornatus* (PIMUZ A/V 439), and *Glyptodon munizi* (PIMUZ A/V 461 and ZMK 69/1885) do not exhibit the same enlarged and ventrally curved area as in *Panochthus intermedius* (ZMK 66/1885) and *Doedicurus clavicaudatus* (see Fig. 5 and ; for Doedicurinae, see Núñez-Blasco et al., 2021). The maxillary bone in the analysed *Neosclerocalyptus* species is laterally elongated compared to the other glyptodonts, a peculiarity underlined by the more posterior position of the orbit and the large additional ossified nasal cartilage on the snout (Fig. 6). In addition, the portion of the maxilla between the descending process of the zygomatic arch and the toothrow has a greater

width in the compared *Neosclerocalyptus* species than in *Panochthus intermedius* (ZMK 66/1885) and *Glyptodon munizi* (PIMUZ A/V 461 and ZMK 69/1885). In the latter and in *Doedicurus clavicaudatus* (PIMUZ A/V 4148), the descending process of the zygomatic arch is more anterolaterally directed with a most lateral position of the tip from the toothrow, contrary to the ventrally directed process of *Panochthus intermedius* (ZMK 66/1885), *Neosclerocalyptus pseudornatus* (PIMUZ A/V 439), and *Neosclerocalyptus gouldi* (ZMK 77/1888). In *Panochthus intermedius* (ZMK 66/1885), *Glyptodon munizi* (PIMUZ A/V 461 and ZMK 69/1885), *Neosclerocalyptus gouldi* (ZMK 77/1888), and *Neosclerocalyptus ornatus* (PIMUZ A/V 447), the palate narrows until the level of Mf3 and then widens anteriorly. In *Neosclerocalyptus pseudornatus* (PIMUZ A/V 439), the toothrows are paralleled, forming an uniform rectangular shape for the palate. Involved in the articulation with the atlas, the two occipital condyles in *Panochthus intermedius* (ZMK 66/1885) are subquadangular, whereas the occipital condyles of *Neosclerocalyptus* species (Zurita et al., 2011b) and *Doedicurus clavicaudatus* (PIMUZ A/V 4148) are subrectangular in cross section and anteroposteriorly elongated. In *Doedicurus clavicaudatus* (PIMUZ A/V 4148), the occipital condyle has nearly the same width as the foramen magnum, while all other genera show a smaller width of the condyle compared to the foramen magnum (Fig. 6 and ; Table 2). *Glyptodon munizi* (PIMUZ A/V 461 and ZMK 69/1885) exhibits the largest and most circular occipital condyle among the discussed species (Fig. 6). The basioccipital and exoccipital in glyptodonts exhibit dozens of basilar tubercles. In *Doedicurus clavicaudatus* (PIMUZ A/V 4148), *Panochthus intermedius* (ZMK 66/1885), and *Glyptodon munizi* (PIMUZ A/V 461 and ZMK 69/1885), the basioccipital is fused with the exoccipital, exhibiting a broad and laterally elongated shape, compared to *Neosclerocalyptus* species, where this region is rather narrow and short. *Doedicurus clavicaudatus* (PIMUZ A/V 4148) exhibits the widest and shortest exoccipital compared to the cranial length, following by a laterally elongated and large foramen magnum (Figs. 6 and 7).

Occipital view

All genera analysed in the present study exhibit a prominent and well-pronounced "W-shaped" nuchal crest joining at the occipital protuberance. In all glyptodonts, the angle between both nuchal crests is larger than 90°, except for *Neosclerocalyptus pseudornatus* (PIMUZ A/V 439) with an angle of only about 90° (Fig. 7). In *Doedicurus clavicaudatus* (PIMUZ A/V 4148), the supraoccipital is subquadangular with a concave surface, whereas other glyptodonts show a more subtriangular shape of

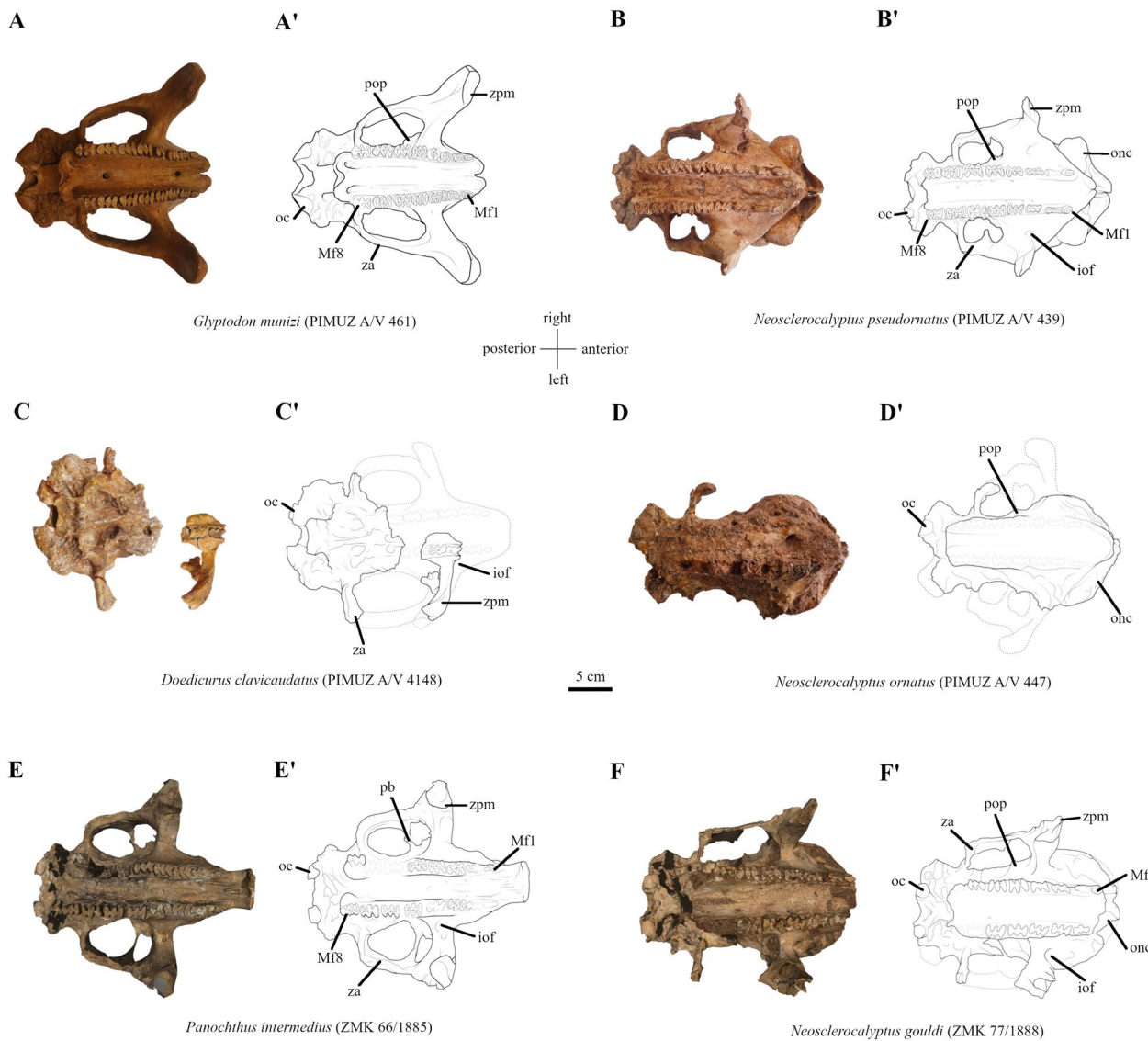


Fig. 6 Plate of the most complete studied crania in ventral view and their associated schematic drawings housed at PIMUZ and ZMK of Pleistocene glyptodonts of the Pampean Region collected by Santiago Roth. iof, infraorbital foramen; Mf1–8, upper molariforms; oc, occipital condyle; onc, ossified nasal cartilage; pb, postorbital bar; pop, postorbital process; za, zygomatic arch; zpm, descending process of the zygomatic arch

the supraoccipital. Among *Neosclerocalyptus* species, *Neosclerocalyptus ornatus* (PIMUZ A/V 447) exhibits the largest laterally expanded supraoccipital. The foramen magnum is smaller and subcircular in *Doedicurus clavicaudatus* (PIMUZ A/V 4148) compared to the *Neosclerocalyptus* species. In the latter, the foramen magnum is subelliptic in cross section, expanding more laterally (see also Zurita et al., 2008). In *Panochthus intermedius* (ZMK 66/1885), the foramen magnum is circular in cross section, same as in other *Panochthus* (Zamorano et al., 2014a). *Glyptodon munizi* (PIMUZ A/V 461 and ZMK 69/1885) exhibits a strong elliptic foramen magnum.

A striking trait observed in *Neosclerocalyptus gouldi* (ZMK 77/1888) and *Neosclerocalyptus pseudornatus* (PIMUZ A/V 439) is that the zygomatic arches (excluding the descending process) are visible in the occipital view, whereas, in the other genera, the zygomatic arches are completely or partially masked by the occiput. The descending process of the zygomatic arch does look similar in *Glyptodon munizi* (PIMUZ A/V 461 and ZMK 69/1885), *Doedicurus clavicaudatus* (PIMUZ A/V 4148; see also Núñez-Blasco et al., 2021), *Neosclerocalyptus pseudornatus* (PIMUZ A/V 439), and *Neosclerocalyptus gouldi* (ZMK 77/1888), exhibiting a straight ventral

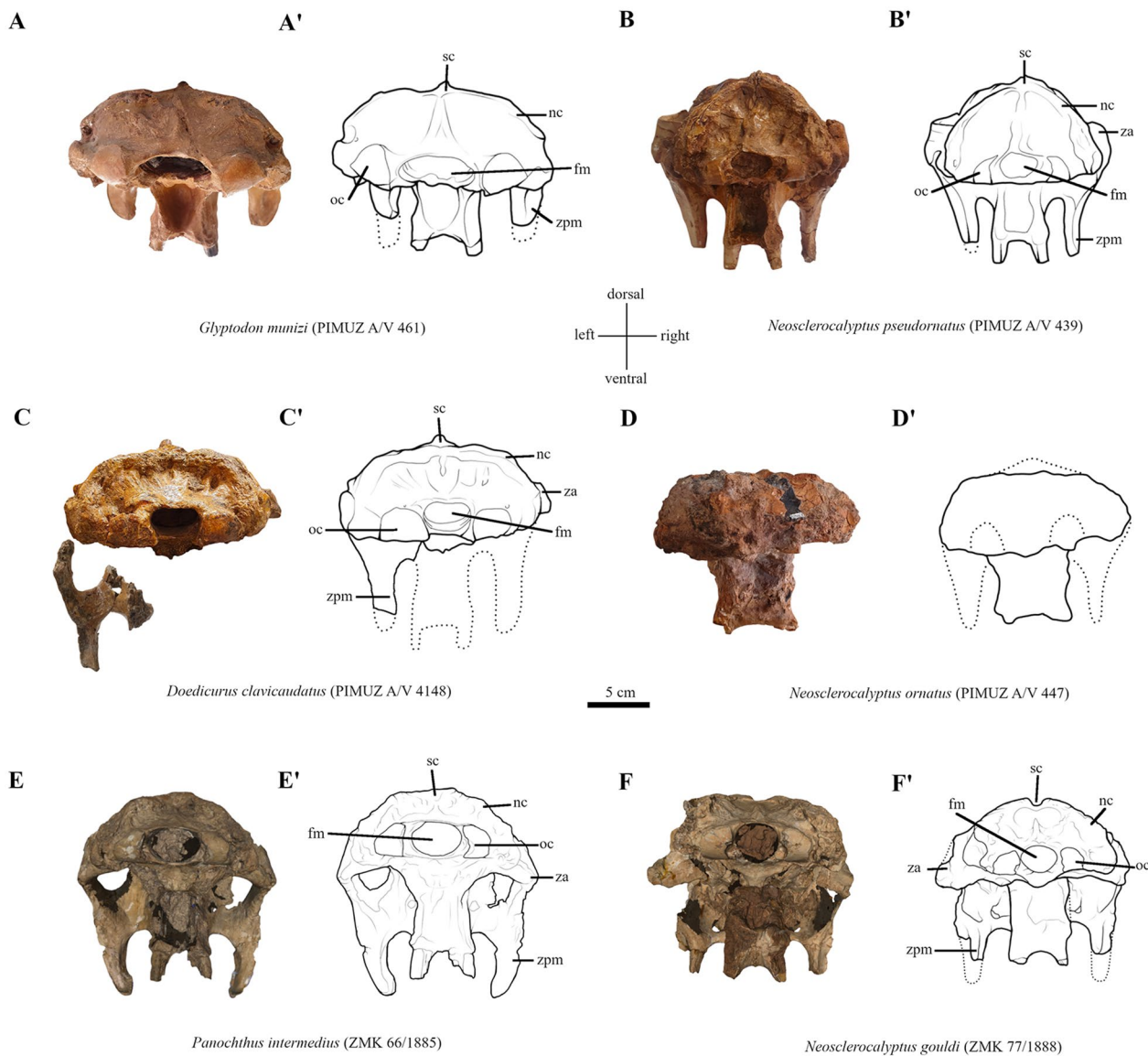


Fig. 7 Plate of the most complete studied crania in occipital view and their associated schematic drawings housed at PIMUZ and ZMK of Pleistocene glyptodonts of the Pampean Region collected by Santiago Roth. fm, foramen magnum; nc, nuchal crest; oc, occipital condyle; sc, sagittal crest; za, zygomatic arch; zpm, descending process of the zygomatic arch

oriented process in occipital view. In *Panochthus intermedius* (ZMK 66/1885) the descending process of the zygomatic arch is tilted slight inwards (Fig. 7).

Mandible

In all genera at the lateral view, toothrows exhibit a sigmoidal course with the posterior end of the toothrow being the most ventral part (Fig. 8). The most dorsal height of the toothrow is at the level of mf3 in *Panochthus intermedius* (ZMK 66/1885), mf2 in *Neosclerocalyptus* species and *Doedicurus clavicaudatus* (Núñez-Blasco et al., 2021), and mf1 in *Glyptodon munizi* (PIMUZ

A/V 461 and ZMK 69/1885). The pre-dentary area in *Doedicurus clavicaudatus* (Núñez-Blasco et al., 2021), *Neosclerocalyptus pseudornatus* (PIMUZ A/V 439), *Neosclerocalyptus gouldi* (ZMK 77/1888), and *Panochthus intermedius* (ZMK 66/1885) lengthens at the most distal part. In *Glyptodon munizi* (PIMUZ A/V 461 and ZMK 69/1885), the pre-dentary area is shorter. The posterior margin of the horizontal ramus is concave in all genera, with the most pronounced curvature expressed in *Doedicurus clavicaudatus* (Núñez-Blasco et al., 2021). In occlusal view, the mandibular symphysis ends at the level of the second lobe of mf4 in *Neosclerocalyptus*

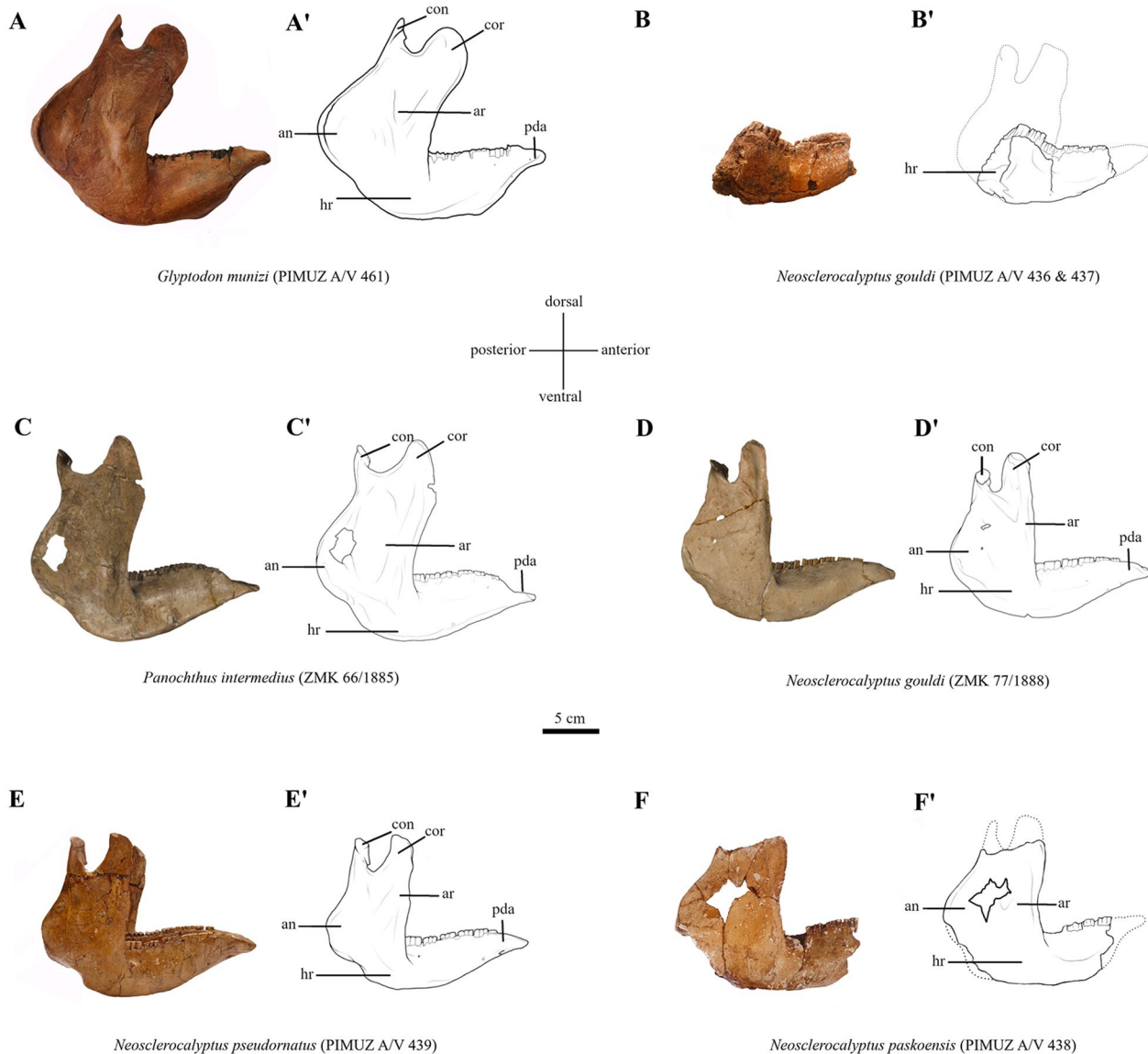


Fig. 8 Plate of the most complete studied mandible in lateral view and their associated schematic drawings housed at PIMUZ and ZMK of Pleistocene glyptodonts of the Pampean Region collected by Santiago Roth. an, angular process; ar, ascending ramus; con, condylar process; cor, coronoid process; hr, horizontal ramus; pda, pre-dentary area

species and *Glyptodon munizi* (PIMUZ A/V 461 and ZMK 69/1885; see also Núñez-Blasco et al., 2021; Soibelzon et al., 2006). In *Panochthus intermedius* (ZMK 66/1885), the mandibular symphysis ends more posteriorly at the level of the second lobe of mf5. The width between the two toothrows is larger in *Glyptodon munizi* (PIMUZ A/V 461 and ZMK 69/1885) than in *Panochthus intermedius* (ZMK 66/1885). In comparison, *Neosclerocalyptus* species exhibits the narrowest relative distance between the lower toothrows. In *Panochthus intermedius* (ZMK 66/1885), this distance widens towards the

posterior end, contrary to *Neosclerocalyptus pseudornatus* (PIMUZ A/V 439), where the distance widens towards the anterior end, and *Glyptodon munizi* (PIMUZ A/V 461 and ZMK 69/1885), *Neosclerocalyptus paskoensis* (Zurita, 2007), and *Neosclerocalyptus gouldi* (ZMK 77/1888) where the toothrows have a subparallel course (Fig. 9). The ascending ramus covers in lateral view the mf7–8 in *Panochthus intermedius* (ZMK 66/1885), mf6–8 in *Neosclerocalyptus* species, and part of the mf5–8 in *Glyptodon munizi* (PIMUZ A/V 461 and ZMK 69/1885) and *Doedicurus clavicaudatus* (Núñez-Blasco

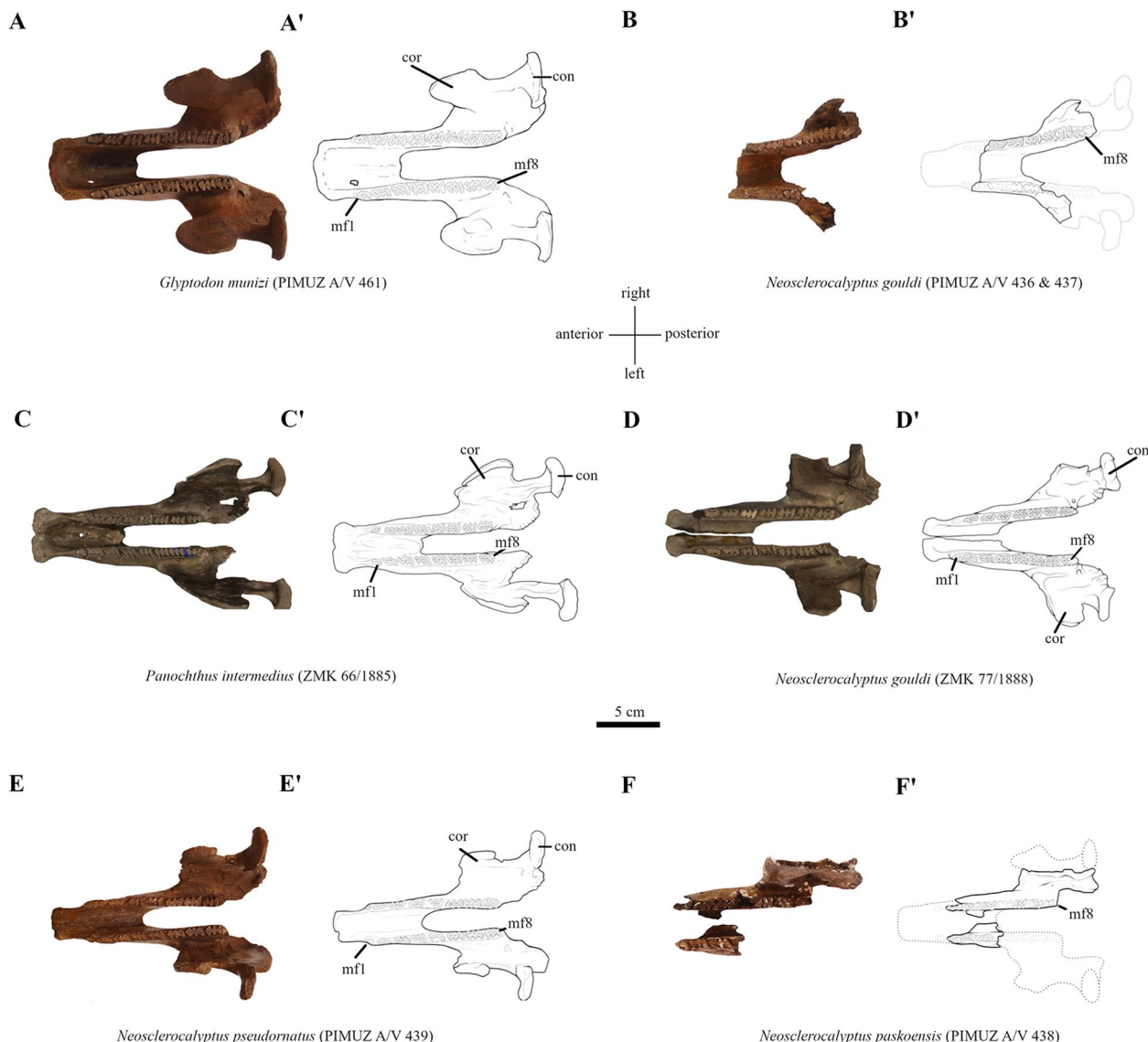


Fig. 9 Plate of the most complete studied mandible in occlusal view and their associated schematic drawings housed at PIMUZ and ZMK of Pleistocene glyptodonts of the Pampean Region collected by Santiago Roth. con, condylar process; cor, coronoid process; mf1–8, lower molariforms

et al., 2021). The approximate angle between the anterior margin of the ascending ramus and the lower toothrow is nearly 90° in *Panochthus intermedius* (ZMK 66/1885), 80°–85° in the *Neosclerocalyptus* (PIMUZ A/V 439, PIMUZ A/V 437 and ZMK 77/1888) species, and 65° in *Glyptodon munizi* (PIMUZ A/V 461) (Table 2). The angular process is concave and round in *Neosclerocalyptus* (Zurita, 2007), Doedicurinae (Núñez-Blasco et al., 2021), and *Panochthus* (Zamorano & Brandoni, 2013), contrary to the subtriangular shape of the angular process in *Glyptodon*. In lateral view, *Glyptodon munizi* (PIMUZ A/V 461 and ZMK 69/1885) also exhibits many tuberosities along the posterior margin of the angular process. The

coronoid process and the condylar process have the same height in *Glyptodon munizi* (PIMUZ A/V 461 and ZMK 69/1885), contrary to the other compared genera, where the coronoid process is higher in lateral view (Fig. 8). The condylar process of all glyptodonts exhibits tuberosities at the anterior margin.

Upper and lower toothrow

Concerning the upper toothrow, all glyptodonts have eight molariforms, the Mf1 being the most variable molar in size and shape. In *Glyptodon munizi* (PIMUZ A/V 461 and ZMK 69/1885) and *Panochthus intermedius* (ZMK 66/1885), the Mf1 shows weak trilobulation, less

lingually marked, whereas in *Doedicurus clavicaudatus* (Núñez-Blasco et al., 2021), and *Neosclerocalyptus* species, the Mf1 has a subcircular and a sub-elliptical cross section, respectively. The pattern of Mf2 shows incipient trilobulation in *Neosclerocalyptus* species, while the Mf2 is already fully trilobated in *Glyptodon munizi* (PIMUZ A/V 461 and ZMK 69/1885) and *Panochthus intermedius* (ZMK 66/1885; Fig. 6). The Mf3 are clearly trilobated in all glyptodont genera and exhibit incipient trilobulation in Doedicurinae (Núñez-Blasco et al., 2021). The first lobes of Mf3 until Mf5 are directed labially, the remaining molariforms are all uniformly trilobated (Núñez-Blasco et al., 2021; Zamorano et al., 2014a; Zurita et al., 2008). The lower toothrow exhibits similar patterns. The mf1 in *Neosclerocalyptus pseudornatus* (PIMUZ A/V 439), *Neosclerocalyptus gouldi* (PIMUZ A/V 77/1888), *Neosclerocalyptus paskoensis* (PIMUZ A/V 438), and Doedicurinae (Núñez-Blasco et al., 2021) are sub-elliptical. In *Glyptodon munizi* (PIMUZ A/V 461 and ZMK 69/1885) and *Panochthus intermedius* (ZMK 66/1885), mf1 are trilobated, but less marked lingually in *Panochthus intermedius* (ZMK 66/1885; Fig. 9). Incipient trilobulation can be distinguished in *Neosclerocalyptus* species and Doedicurinae (Núñez-Blasco et al., 2021) from the mf2, whereas, in *Panochthus intermedius* (ZMK 66/1885) and *Glyptodon munizi* (PIMUZ A/V 461 and ZMK 69/1885), the mf2 are already fully trilobated. From mf3 to mf8, the trilobulation proximally increases in all genera, exhibiting an increased tilt to the lingual side of each last lobe. In *Panochthus intermedius* (ZMK 66/1885) and *Glyptodon munizi* (PIMUZ A/V 461 and ZMK 69/1885), the last lobe of the mf8 is tilted outwards (Fig. 9).

Endocranial anatomical comparison

Inner ear

All described species display a poorly coiled cochlea, one with just 1.5 turns (Fig. 10). Specimens exhibit large semicircular canals in proportion to the cochlea and an overall relatively small size of the inner ear compared to the size of the cranium (see below). The semicircular canals in *Neosclerocalyptus pseudornatus* (PIMUZ A/V 439) are more rounded than in the other species studied. In *Glyptodon munizi* (PIMUZ A/V 461) the semicircular canals exhibit an oval shape. In contrast with other glyptodonts, *Doedicurus clavicaudatus* (PIMUZ A/V 4148) shows a small lateral semicircular canal compared to the anterior and posterior semicircular canals. In this specimen, the anterior and posterior semicircular canals are equal in size, whereas in smaller glyptodonts, such as *Glyptodon* species (Fariña et al., 1998), the posterior semicircular canal is larger compared to the remaining semicircular canals (Fig. 10; Table 2). As a glyptodont closer in size to

Doedicurus clavicaudatus than *Glyptodon* species (Fariña et al., 1998), *Panochthus tuberculatus* exhibits a larger lateral semicircular canal compared to the anterior semicircular canal (Tambusso et al., 2021). *Neosclerocalyptus pseudornatus* (PIMUZ A/V 439) shows similar sizes of all semicircular canals (Table 2). Regarding the relative position of each semicircular canal, *Glyptodon munizi* (PIMUZ A/V 461) shows a more acute angle dorsal to the *crus commune* between anterior and posterior semicircular canal than *Doedicurus clavicaudatus* (PIMUZ A/V 4148), *Neosclerocalyptus pseudornatus* (PIMUZ A/V 439; Fig. 10), and *Panochthus tuberculatus* (Tambusso et al., 2021; Table 2). The *crus commune*, formed by the merge of the anterior and posterior semicircular canals, is thinner in *Doedicurus clavicaudatus* (PIMUZ A/V 4148) than in the remaining glyptodonts. This result should be moderated as the *crus commune* appears relatively equivalent in size in all glyptodonts in the studies of Tambusso et al., (2021, 2023), underlining a potential intraspecific variation of the *crus commune* thickness in *Doedicurus*. The angle between posterior part of lateral and posterior semicircular canals in *Glyptodon munizi* (PIMUZ A/V 461) is smaller than in *Doedicurus clavicaudatus* (PIMUZ A/V 4148) and *Neosclerocalyptus pseudornatus* (PIMUZ A/V 439). In *Neosclerocalyptus pseudornatus* (PIMUZ A/V 439), these two semicircular canals only meet in the utricle, a feature also found in the Miocene glyptodont *Pseudolophophorus* (Tambusso et al., 2021, 2023), whereas in the remaining species they already meet more anteriorly, forming the secondary common *crus*. Therefore, the anterior and lateral ampulla in *Neosclerocalyptus pseudornatus* (PIMUZ A/V 439) are well-separated by a gap, formed by the more anterior connection of their ampulla, in comparison with the remaining species. From the dorsal view (Fig. 10A–F), *Doedicurus clavicaudatus* (PIMUZ A/V 4148) exhibits a steeper connection of the posterior semicircular canal and the posterior ampulla compared to *Glyptodon munizi* (PIMUZ A/V 461) and *Neosclerocalyptus pseudornatus* (PIMUZ A/V 439), for which this connection is more horizontal and rounded downwards. Compared to *Glyptodon munizi* (PIMUZ A/V 461) and *Neosclerocalyptus pseudornatus* (PIMUZ A/V 439), *Doedicurus clavicaudatus* (PIMUZ A/V 4148) displays a more ventrally positioned cochlea with respect to the endolymphatic duct, a position associated with a more ventrally tilted basal cochlear turn in *Doedicurus clavicaudatus* (PIMUZ A/V 4148; see also for *Chlamyphorus* in Billet et al. (2015a) and for *Glyptodon* in Tambusso et al. (2021)). In anterior view, the rest of the cochlea is more upwardly directed in *Doedicurus clavicaudatus* (PIMUZ A/V 4148) and in *Neosclerocalyptus pseudornatus* (PIMUZ A/V 439) than in *Glyptodon*

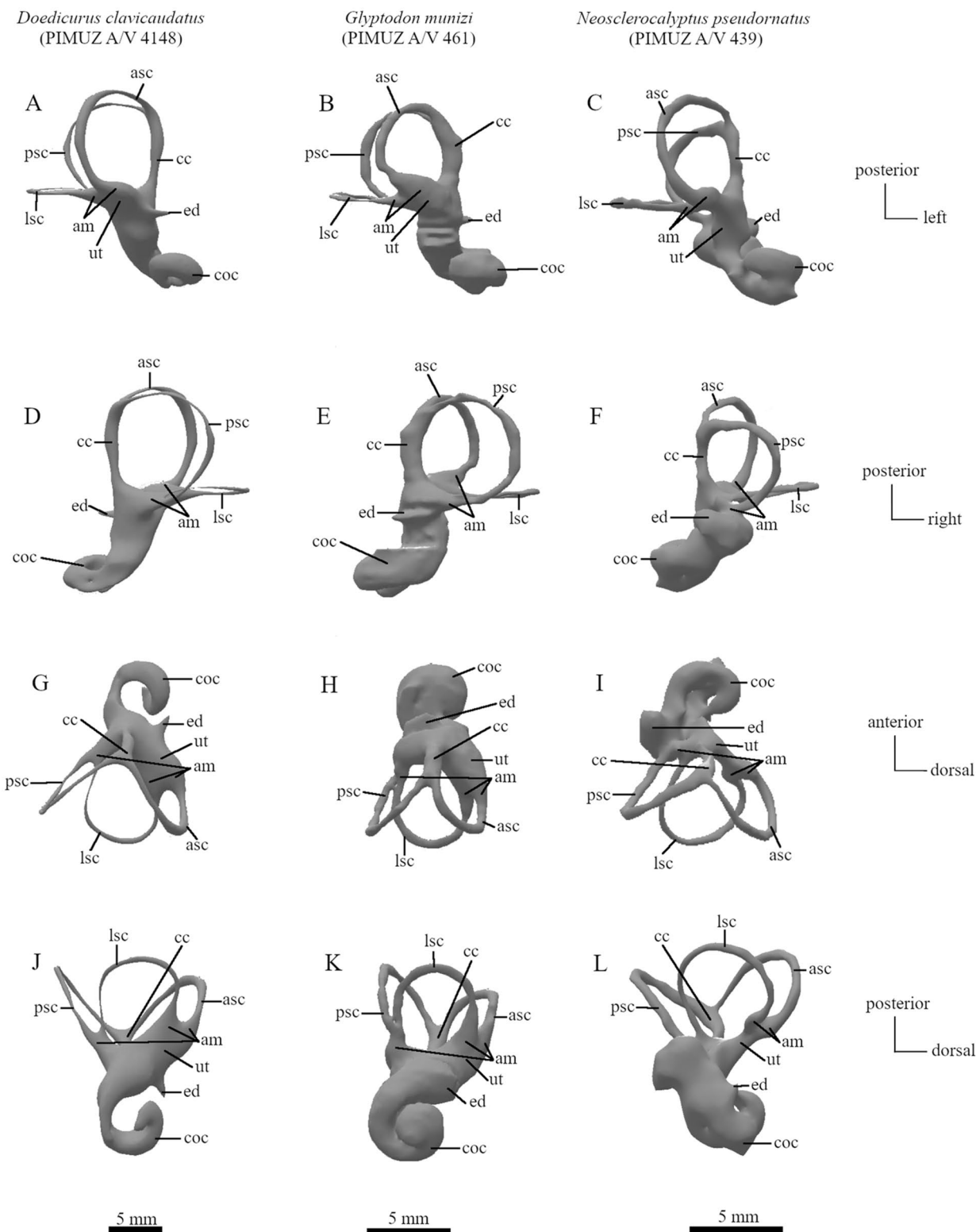


Fig. 10 Plate of the reconstructed inner ear including *Doedicurus clavicaudatus*, *Glyptodon munizi*, and *Neosclerocalyptus pseudornatus*. am, ampulla; asc, anterior semicircular canal; cc, crus commune; coc, cochlea; ed, endolymphatic duct; lsc, lateral semicircular canal; psc, posterior semicircular canal; ut, utricle

munizi (PIMUZ A/V 461), in which the cochlea is oriented horizontally (Fig. 10).

Braincase

The digital braincase of *Doedicurus clavicaudatus* (PIMUZ A/V 4148), *Glyptodon munizi* (PIMUZ A/V 461), and *Neosclerocalyptus pseudornatus* (PIMUZ A/V 439) are almost complete and well-preserved. The cerebellar hemispheres are more laterally expanded in the larger species *Doedicurus clavicaudatus* (PIMUZ A/V 4148), *Panochthus tuberculatus* (Tambusso & Fariña, 2015a), and *Glyptodon munizi* (PIMUZ A/V 461) compared to *Neosclerocalyptus pseudornatus* (PIMUZ A/V 439), leading to a more anteroposterior elongated cerebellum in the latter (Fig. 11), a feature also found in *Pseudoplophorus* (Tambusso & Fariña, 2015a; Tambusso et al., 2023). In all specimens, the strongly pronounced vermis does not form any kind of posterior apex. The digital braincase of *Neosclerocalyptus pseudornatus* (PIMUZ A/V 439) exhibits a proportionally larger cerebellum compared to the other species, but also exhibits a similar size of the cerebrum, while having atrophied olfactory bulb compared to *Doedicurus clavicaudatus* (PIMUZ A/V 4148), *Panochthus tuberculatus* (Tambusso & Fariña, 2015a), and *Glyptodon munizi* (PIMUZ A/V 461). Like the cerebrum, in anterior view, the olfactory bulbs of *Glyptodon munizi* (PIMUZ A/V 461) are more dorsoventrally elongated than in *Doedicurus clavicaudatus* (PIMUZ A/V 4148), but both species exhibit the same frontal orientation of the olfactory bulbs. In *Neosclerocalyptus pseudornatus* (PIMUZ A/V 439), the olfactory bulbs are smaller than in the remaining species in relation to the braincase size, and are situated at the ventral edge of the cerebrum. The ventral position of the olfactory bulbs in *Neosclerocalyptus pseudornatus* (PIMUZ A/V 439) implies a relatively larger longitudinal sulcus in the anterior view. *Panochthus tuberculatus* shows a similar relative size of olfactory bulbs (Tambusso & Fariña, 2015a) to *Glyptodon munizi* (PIMUZ A/V 461) and *Doedicurus clavicaudatus* (PIMUZ A/V 4148), situated at the ventral edge of the cerebrum, like in *Neosclerocalyptus pseudornatus* (PIMUZ A/V 439) but more laterally oriented in dorsal view in the latter (Tambusso & Fariña, 2015a). In lateral view, with respect to the medulla oblongata, the cerebrum is slightly inclined ventrally in *Neosclerocalyptus pseudornatus* (PIMUZ A/V 439) and *Panochthus tuberculatus* (Tambusso & Fariña, 2015a), inclined dorsally in *Doedicurus clavicaudatus* (PIMUZ A/V 4148), and even more inclined dorsally in *Glyptodon munizi* (PIMUZ A/V 461). In the latter, the mediolaterally oriented occipital gyrus at the border between the cerebrum and the cerebellum is more prominently concave than in *Doedicurus clavicaudatus* (PIMUZ A/V

4148) and *Neosclerocalyptus pseudornatus* (PIMUZ A/V 439), leading to a more pronounced transverse fissure in *Glyptodon munizi* (PIMUZ A/V 461). The cerebral hemispheres in dorsal view are separated by a strongly protruding medial part of the lateral gyrus, which is thinner and extends over the entire length of the cerebrum in *Doedicurus clavicaudatus* (PIMUZ A/V 4148) and *Neosclerocalyptus pseudornatus* (PIMUZ A/V 439) compared to *Glyptodon munizi* (PIMUZ A/V 461) and *Panochthus tuberculatus* (Tambusso & Fariña, 2015a). For the latter, this part of the gyrus is more pronounced and only visible in the posterior and most anterior part of the cerebrum. In *Glyptodon munizi* (PIMUZ A/V 461), *Panochthus tuberculatus* (Tambusso & Fariña, 2015a), and *Neosclerocalyptus pseudornatus* (PIMUZ A/V 439), the lateral portion of the lateral gyrus is well-preserved and, on both hemispheres, anteroposteriorly directed and more pronounced compared to *Doedicurus clavicaudatus* (PIMUZ A/V 4148). The suprasylvian gyrus, situated laterally to the lateral gyri, is not prominent in all species. *Glyptodon munizi* (PIMUZ A/V 461) and *Doedicurus clavicaudatus* (PIMUZ A/V 4148) exhibit a defined temporal and pyriform lobe, whereas in *Neosclerocalyptus pseudornatus* (PIMUZ A/V 439), the two lobes are less protruding in lateral and dorsal views, which leads to a more quadrangular and narrower cerebrum in anterior view (Fig. 11). In this latter view, *Doedicurus clavicaudatus* (PIMUZ A/V 4148) exhibits a similar shape to that in *Glyptodon munizi* (PIMUZ A/V 461), with a less dorsoventral elongation of the cerebrum. *Neosclerocalyptus pseudornatus* (PIMUZ A/V 439) and *Panochthus tuberculatus* (Tambusso & Fariña, 2015a) show a prominent fissure between the olfactory gyrus and the pyriform lobe viewed from the dorsal side that is not as strongly visible in *Doedicurus clavicaudatus* (PIMUZ A/V 4148) and *Glyptodon munizi* (PIMUZ A/V 461). The olfactory gyrus is anteroposteriorly elongated in *Neosclerocalyptus pseudornatus* (PIMUZ A/V 439).

Related cranial canals

In *Neosclerocalyptus pseudornatus* (PIMUZ A/V 439), the posttemporal canal runs dorsally to the level of the internal auditory meatus from the outreaching flanks of the cerebellum. In *Glyptodon munizi* (PIMUZ A/V 461) and *Doedicurus clavicaudatus* (PIMUZ A/V 4148), the posttemporal canal emerges posteroventrally to the internal auditory meatus (Fig. 11). In all species, the ventral part of the posttemporal canal exhibits a downward trajectory. In lateral view, the posttemporal canal is oriented vertically in *Doedicurus clavicaudatus* (PIMUZ A/V 4148) and *Neosclerocalyptus pseudornatus* (PIMUZ A/V 439), in contrast to the more posterodorsal orientation in *Glyptodon munizi* (PIMUZ A/V 461). In anterior

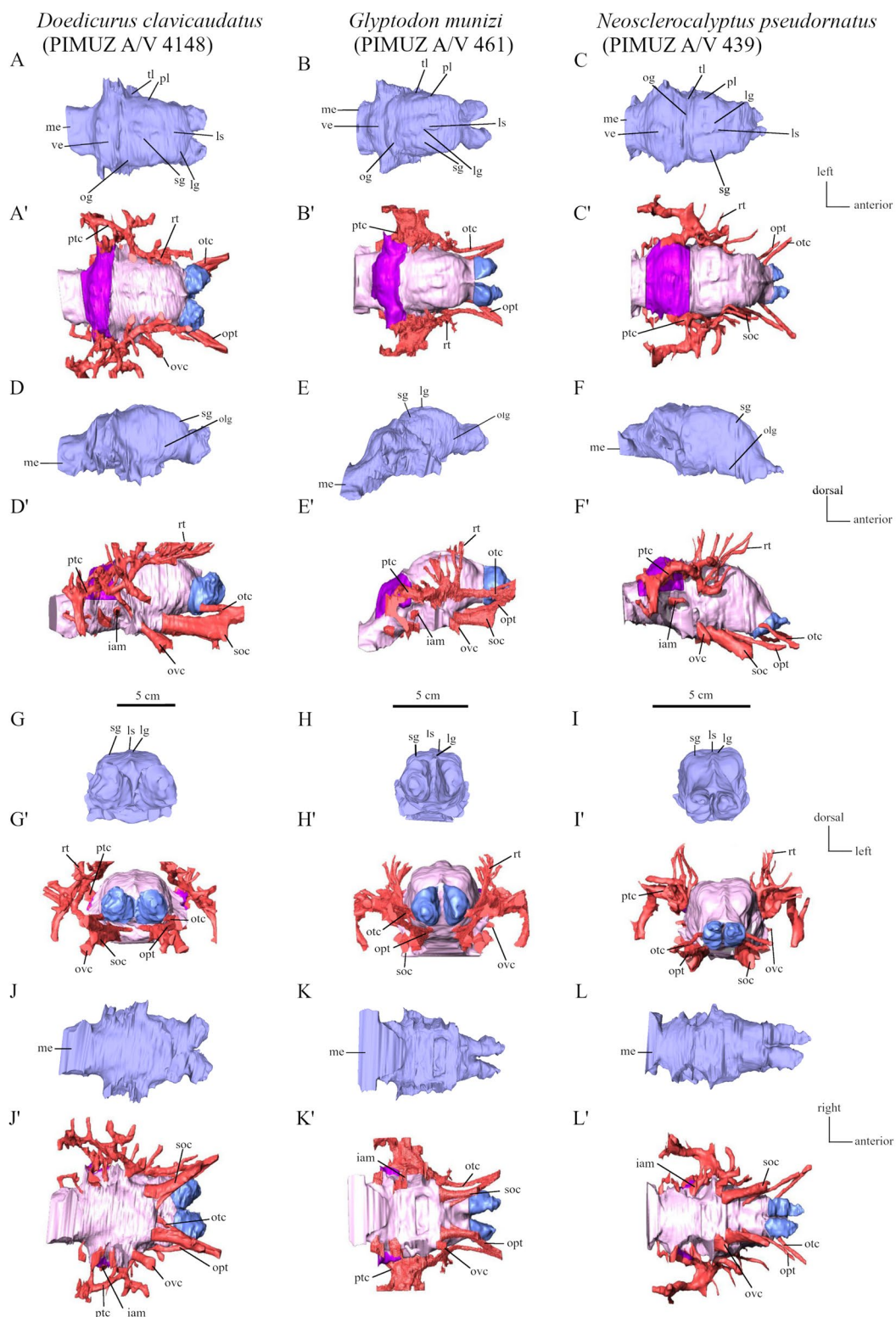


Fig. 11 Plate of the reconstructed braincase (blue—olfactory bulbs; pink—cerebrum and brain stem (pons + medulla oblongata); purple—cerebellum) and associated canals (red) including *Doedicurus clavicaudatus*, *Glyptodon munizi*, and *Neosclerocalyptus pseudornatus*. *iam*, internal auditory meatus; *lg*, lateral gyrus; *ls*, longitudinal sulcus; *me*, medulla oblongata; *og*, occipital gyrus; *olg*, olfactory gyrus; *opt*, optic canal; *otc*, orbitotemporal canal; *ovc*, oval canal; *ptc*, post temporal canal; *rt*, rami temporales; *sg*, suprasylvian gyrus; *soc*, sphenorbital canal; *tl*, temporal lobe; *ve*, vermis

view, the descending branch of the posttemporal canal is directed outwards for *Doedicurus clavicaudatus* (PIMUZ A/V 4148) and *Neosclerocalyptus pseudornatus* (PIMUZ A/V 439) whereas for *Glyptodon munizi* (PIMUZ A/V 461) this canal displays an inwards curvature (Fig. 11). The posttemporal canal in *Neosclerocalyptus pseudornatus* (PIMUZ A/V 439) exhibits a strong ventral curvature until the level of the oval canal. According to Wible and Gaudin (2004), this canal transmits the *arteria diploëtica magna* and the large *vena diploëtica magna*. Along the lateral side of all braincases, the posttemporal canal connects to a confluence area as described in Le Verger et al. (2021) (see below). The *rami temporales* observed in all species open in the cranial roof in various foramina (e.g., Gaudin & Wible, 2006), marking auxilliary canals from the main braincase canals for the vascularization of *temporalis* muscles, here, emerging mainly from the orbitotemporal canal (Fig. 11; see Le Verger et al., 2021 for more details in glyptodonts, and MacPhee et al., 2021 for different origins of *rami temporales* in mammals). The largest glyptodont, *Doedicurus clavicaudatus* (PIMUZ A/V 4148), exhibits a high density and broad canals of the *rami temporales* in contrast to the remaining species. *Neosclerocalyptus pseudornatus* (PIMUZ A/V 439) shows a relatively similar number of *rami temporales* as *Glyptodon munizi* (PIMUZ A/V 461). Le Verger et al. (2021) described a region of confluence between the orbitotemporal canal, the canal for the capsuloparietal emissary vein, and the posttemporal canal, where the canals can no longer be distinguished from each other, a region well-defined in *Doedicurus clavicaudatus* (PIMUZ A/V 4148) and *Glyptodon munizi* (PIMUZ A/V 461; Fig. 11). *Glyptodon munizi* (PIMUZ A/V 461) stands out concerning the course of the orbitotemporal canal, since it horizontally follows the lateral wall of the cranial roof until it connects to the optic canal, unlike in *Neosclerocalyptus pseudornatus* (PIMUZ A/V 439) and *Doedicurus clavicaudatus* (PIMUZ A/V 4148) where the orbitotemporal canal provide a passage through the braincase. The orbitotemporal canal transmits the orbitotemporal artery and accompanying vein (e.g., MacPhee et al., 2021) and parts of the *ramus superior* of the stapedial artery (Wible & Gaudin, 2004). In *Glyptodon munizi* (PIMUZ A/V 461) and *Doedicurus clavicaudatus* (PIMUZ A/V 4148), the sphenorbital and optic canals are connected to the orbitotemporal canal. The connection with respect to the anterior end of the olfactory bulb is more anterior in *Doedicurus clavicaudatus* (PIMUZ A/V 4148) than in *Glyptodon munizi* (PIMUZ A/V 461). In lateral view, the sphenorbital canal is directed, with respect to the transverse plane, anteriorly in *Glyptodon munizi* (PIMUZ A/V 461), anteroventrally in *Doedicurus clavicaudatus* (PIMUZ A/V 4148) and even more ventrally in *Neosclerocalyptus*

pseudornatus (PIMUZ A/V 439), this variation being perhaps correlated with the difference in orientation of the brain among the species. The distance in ventral view between the sphenorbital canal and the oval canal is especially larger in *Doedicurus clavicaudatus* (PIMUZ A/V 4148), following the observed trend of their overall larger canals. The sphenorbital canal transmits the ophthalmic and maxillary branches of the trigeminal nerve, oculomotor, trochlear, and abducens nerves, with accompanying veins, and a small branch of the maxillary artery which open in the sphenorbital fissure (Boscaini et al., 2020a; Le Verger et al., 2021; Wible & Gaudin, 2004). Moreover, in *Doedicurus clavicaudatus* (PIMUZ A/V 4148), the oval canal, which transmits the mandibular division of the trigeminal nerve (see for sloths Boscaini et al., 2020b), is directed more laterally in anterior view than in the remaining specimens. The optic canal opens externally at the optic foramen and connects to the encephalic cavity, located ventrally in the cerebrum. In *Doedicurus clavicaudatus* (PIMUZ A/V 4148), the two openings of the optic canal are closer together in anterior view than in *Glyptodon munizi* (PIMUZ A/V 461) and *Neosclerocalyptus pseudornatus* (PIMUZ A/V 439), a trend that could potentially be an allometric effect, as inferred from a study on *Dasypus* (Le Verger et al., 2020). The optic nerve, the internal ophthalmic artery, and the internal ophthalmic vein are transmitted through the optic canal (Wible & Gaudin, 2004). The internal auditory meatus, bearing the facial and vestibulocochlear nerves (Boscaini et al., 2020b; Wible, 2010), are situated ventrally to the anterior part of the cerebellum in all species. The vestibulocochlear nerves split into the vestibular and cochlear nerve and open at the level of the inner ear region (Tambusso & Fariña, 2015a; Wible & Gaudin, 2004). In *Neosclerocalyptus pseudornatus* (PIMUZ A/V 439) and *Doedicurus clavicaudatus* (PIMUZ A/V 4148), the well-marked bifurcation of this canal into the vestibular and cochlear part can be observed (Fig. 11).

Discussion

Glyptodont diversity has been overestimated for the Pleistocene, and following several taxonomic revisions, some authors now suggest a decline in the Pleistocene glyptodont diversity probably due to several causes, related to the increase in body size, different latitudinal distribution of the genera, or the drastic climatic changes during this period (Cuadrelli et al., 2019, 2020; Vizcaíno et al., 2012; Zurita et al., 2016, 2018). The Pampean Region marks the ecoregion between the tropical and the temperate/arid ecosystems associated with a high productivity related to the Paleo-Parana River floods (Varela & Fariña, 2016; Varela et al., 2018), a region inhabited by the southern glyptodont taxa. Two radiations within the

glyptodont have been identified (e.g., Núñez-Blasco et al., 2021). One corresponds to the Hoplophorinae, a clade notably formed by the grouping of *Panochthus* and *Neosclerocalyptus*, two genera including eight species and four species during this period, respectively (Zamorano et al., 2021; Zurita et al., 2011b). The second correspond to the Glyptodontinae, which, during the Pleistocene, consisted only of the genus *Glyptodon*, restricted to South America, and the genus *Glyptotherium* Osborn, 1903, more widely distributed in North America and in northern South America (Zurita et al., 2018). In current phylogenies of Pleistocene glyptodonts, either *Doedicurus* is the sister group of the Hoplophorinae and the group they form is positioned as the sister group of the Glyptodontinae (Núñez-Blasco et al., 2021), or *Doedicurus* and *Glyptodon* form one clade and *Neosclerocalyptus* and *Panochthus* form another one (Fernicola et al., 2018). We base the following discussion of potential and optimized characters from our comparative analysis on these two phylogenetic hypotheses.

The most recent phylogenetic matrix used to address the evolutionary history of glyptodonts has 57 characters for 27 taxa and includes the four major Pleistocene glyptodont genera. Among the 57 characters, 20 are defined on the skull, including the dentition. Only five of these characters provide hypotheses of homologies among genera and not always in agreement with the topology obtained in the strict consensus (Fig. 12 and Núñez-Blasco et al., 2021), implying that phylogeny at the scale of glyptodont genera is based mainly on postcranial material. We propose potential new cranial and endocranial characters to support different phylogenetic scenarios: 17 new characters could be defined based on the work we present (Fig. 12). In agreement with the monophyly of Hoplophorinae and the position as sister group of *Doedicurus* with the latter, supported in previous studies only by the presence of a pneumatization of the rostral region in *Neosclerocalyptus* and *Panochthus* (K2*) and the onset of labiolingual trilobulation at Mf2 in *Neosclerocalyptus* and *Panochthus* and Mf3 in *Doedicurus*, we propose seven new potential synapomorphies, five of which concern the general shape of the cranium (K1–K5), one corresponds to the lower dentition (K6), and one is defined by the inclination of the cerebrum (K14). Of these seven potential synapomorphies, six could also support the alternative phylogenetic hypothesis proposing closer relationship between the *Glyptodon* and *Doedicurus* (K1, K3–6, K14; Fernicola et al., 2018). Consequently, most of the potential external cranial characters studied here, and the unique character on the cerebrum, do not resolve between the phylogenetic hypothesis of Núñez-Blasco et al. (2021) and that of Fernicola et al. (2018).

Regarding other potential external cranial characters, we hypothesize on morphological convergences among glyptodonts, including the absence or presence of a curvature of the cranial roof (K9) and the descending process of the zygomatic arch (K10), grouping *Doedicurus* and *Neosclerocalyptus* each, and also supported by a subelliptic shape of the orbit (K11). Based on the trend of a more convergent orbit orientation in larger species such as *Doedicurus*, *Panochthus* and *Glyptodon* compared to *Neosclerocalyptus*, a diverse range of vision from a dominance of a monocular to binocular visual field in relation to size variation in Pleistocene glyptodonts is supported. This would mark a well-known allometric variation in mammals (Heesy, 2004, 2008). *Neosclerocalyptus* exhibit a smaller and more posterior situated orbit in lateral view, probably due to the development of the prominent ossified nasal cartilage (Zurita et al., 2011b). *Doedicurus* also appear to have potential morphological convergences with the *Panochthus*, both clades sharing a strong protrusion of the zygomatic process of the squamosal (K7) and a circular shape of the foramen magnum (K8). The last two characters (K7 and K8) could be related to the allometric effect, since *Doedicurus* and *Panochthus* share a significantly larger body mass (~1400 kg up to ~2000 kg; Fariña, 1995; Fariña et al., 1998) than the small *Neosclerocalyptus* (~320 kg; Vizcaíno et al., 2011). In addition to the presence of an ossified nasal cartilage in *Neosclerocalyptus*, a strong impact of allometry was demonstrated in one extant armadillo species, *Dasypus novemcinctus* Linnaeus, 1758, leading to a protrusion of the zygomatic process of the squamosal and a modification of the shape of the foramen magnum (Le Verger et al., 2020). For these two traits, a potential correlation with size must be explored to evaluate if they are impacted by allometry or phylogenetic characters independent of size. The ossified nasal cartilage in *Neosclerocalyptus* species and the elongated nasal bone in *Panochthus intermedius* enlarges the snout area, and therefore, the position of the orbit is in the middle portion of the cranium. Pleistocene glyptodonts show great diversity in snout shape. This diversity has been associated with the respiratory and thermoregulatory functions of the nasal cavity in relation to the changing climatic cycles between glacial and interglacial that occurred during the Pleistocene (e.g., Rabassa & Coronato, 2009; Rabassa et al., 2005) and the potential low metabolic rate of glyptodonts (Vizcaíno et al., 2006), especially in the case of the *Neosclerocalyptus* (Zurita et al., 2011b), although this hypothesis is disputed (Fernicola et al., 2012). Our search for homology hypotheses was limited by the *Neosclerocalyptus* with the presence of the most unique external cranial traits, which may be closely linked to the presence of the prominent ossified nasal cartilage (Fernicola et al., 2012). This applies

especially to *Neosclerocalyptus pseudornatus*, which shows most of the morphological differences in relation to the rest of the *Neosclerocalyptus* species. Anagenesis has been accepted concerning the evolution of the genus *Neosclerocalyptus* (e.g., Quiñones et al., 2020; Zurita et al., 2011b), but PIMUZ A/V 439 exhibits some unique characters which differ vastly from the remaining *Neosclerocalyptus* species and would mark a clear morphological differentiation between the early forms of the Ensenadan Stage and those from the Lujanian Stage.

The four Pleistocene glyptodontid genera, *Doedicurus*, *Glyptodon*, *Panochthus*, and *Neosclerocalyptus*, co-occurred in the “Pampean Formation” of Argentina, with ecological niche partitioning among them (e.g., De Melo-Franca et al., 2015; Domingo et al., 2012; Vizcaíno et al., 2011) and some of the characters mentioned above might be common morphological trait acquisitions related to the paleoenvironmental evolution of the region. For instance, *Doedicurus clavicaudatus* and *Panochthus intermedius* both inhabited the Pampean Region during the late Ensenadan/Bonaerian (see Table 1); these two genera show many common adaptational features related to the similar environmental conditions during the Bonaerian of the Pampean Region, a period that started with a great warming and suffered a severe cooling of the climate (Quattroccchio et al., 2008; Soibelzon, 2019). The acquisition of certain synapomorphies such as the round shape of the cranium in anterior view (K1) and the narial opening (K2) or the pneumatization of the rostral area (K2*) were notably hypothesized to be related to the cooling phases and the aridity of the climate during the Pleistocene (Fernicola et al., 2012; Zurita et al., 2011a), characters supporting the clade formed by *Neosclerocalyptus* and *Panochthus*. There may be an adaptive value for some of the new characters, as in the position of the head and the cranial roof, suggesting a larger area for muscle attachment (e.g., K3 and K5), related to wide muzzles and high hypsodonty index, typical features of bulk feeding in open environments (Vizcaíno et al., 2011). The hypothesis of a strong plasticity associated with dietary changes seems supported by the isotopic analyses on the diet of *Glyptodon* that showed a mixture

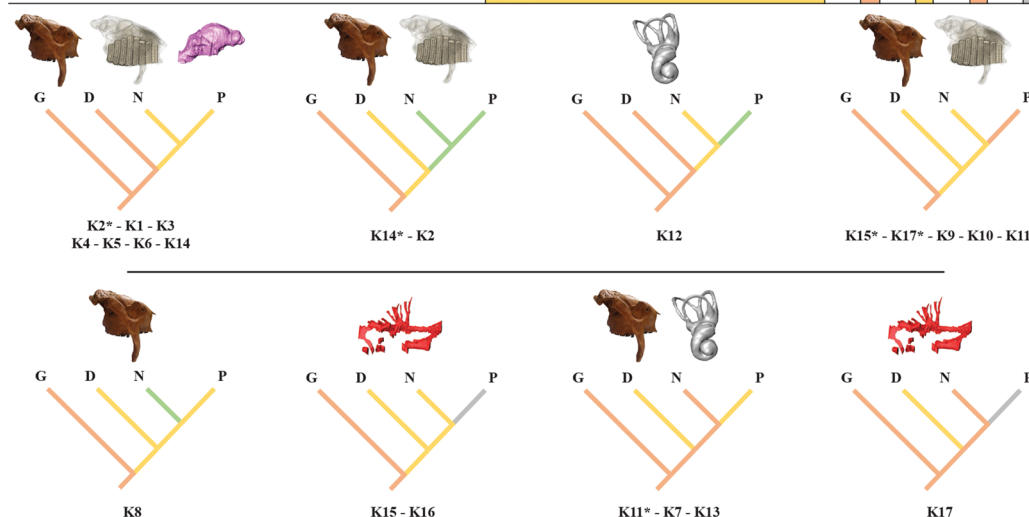
of a C3 and C4 plant diet or a solely C3 plant diet, reflecting ecological plasticity (Cuadrelli et al., 2020; Domingo et al., 2012; Prado et al., 2011). However, the majority of other glyptodont genera have been interpreted as specialized (Vizcaíno et al., 2011) with the assignment of *Doedicurus* and *Panochthus* to bulkfeeders in open environments and *Neosclerocalyptus* to bulkfeeders in closer environments. The conspicuous trilobulation morphology observed in *Glyptodon munizi* is a synapomorphy of the genus (Cuadrelli et al., 2020; Zurita et al., 2013). Some of our characters such as those grouping *Doedicurus* and *Panochthus* may be the result of feeding strategy specializations and any hypothesis of synapomorphy should be considered with caution as the radiation of each genus occurred before the Pleistocene (Nuñez-Blasco et al., 2021; Zamorano et al., 2014b).

We recorded differences in the studied endocranial structures among *Glyptodon munizi*, *Neosclerocalyptus pseudornatus*, *Panochthus tuberculatus* (Tambusso & Fariña, 2015a), and *Doedicurus clavicaudatus*. Overall, the braincase of *Doedicurus clavicaudatus* and *Glyptodon munizi* share more morphological similarities among the analysed braincase endocasts than with *Neosclerocalyptus pseudornatus*, supporting the phylogenetic hypothesis of Fernicola et al. (2018). First, regarding proportions of different braincase regions, the relative volume of the cerebellum is smaller in *Doedicurus clavicaudatus* compared to the other species (Table 2), implying a lesser development of the brain in this genus for sensory control of movement (Sultan & Glickstein, 2007). In *Glyptodon munizi*, the relative volume for the cerebrum, the cerebral neocortex involved in several perceptual and cognitive functions (Van Essen, 1979), is smaller than in *Neosclerocalyptus pseudornatus* and *Doedicurus clavicaudatus* (Table 2). Based on the analyses of Stankowich & Romero (2017), mammals living in open environments and with external antipredator defenses show reduced encephalization, since these defense strategies reduce the need of spending production and maintenance costs of cognitive abilities related to vigilance and predator recognition. These analyses are in accordance with our results on *Glyptodon munizi* showing a relative

(See figure on next page.)

Fig. 12 Former and new potential phylogenetic characters for the relationships among the Pleistocene glyptodont genera from our comparative investigation. Shared morphological traits are defined as characters in the illustrated table and each homological or homoplasical hypothesis is illustrated on the schematic tree extracted from the strict consensus of Nuñez-Blasco et al. (2021) to address the evolutionary history of glyptodonts. For each evolutionary scenario, the anatomical regions involved are identified by a symbol from the cranium of *Glyptodon munizi* (PIMUZ A/V 461) in lateral view: a cranium for external morphological features, a cranium in transparency with teeth selected for dental characters, an isolated braincase endocast, an isolated and verticalized inner ear, and the neurocranial canals. The color follows the coding of each character. See Table 2 for measurement abbreviations. Symbol: *, from Nuñez-Blasco et al. (2021). D, *Doedicurus*; G, *Glyptodon*; K, character; N, *Neosclerocalyptus*; P, *Panochthus*

Previous Character (=KX*)	States	G	D	N	P
K2*: Rostral area pneumatization	0: Absent 1: Present	0	0	1	1
K11*: Palate morphology	0: Transverse expansion absent or limited to one margin 1: Transverse expansion in its distal and proximal margins	0	1	0	1
K14*: Labiolingual trilobation begins	0: Mf1 or Mf2 1: Mf3 2: Mf2	0	1	2	2
K15*: Labio-lingual axis of the Mf1 ≥ 75% of the anteroposterior axis	0: Absent 1: Present	0	1	1	0
K17*: Morphology of the Mf2/mf2	0: Scarcely lobulated in both margins 1: Scarcely lobulated, particularly of the lingual margin	0	1	1	0
Potential New Character (=KX)	States	G	D	N	P
K1: Anterior cranial shape	0: Subrectangular 1: Round	0	0	1	1
K2: Narial opening shape	0: Subtriangular 1: Rectangular 2: Round or hooded	0	1	2	2
K3: Angle between SP and TP	0: <45° 1: >45°	0	0	1	1
K4: MOC vs MFMW	0: MOC larger 1: MOC smaller	0	0	1	1
K5: Basicranial position related to orbital dorsal margin	0: Dorsal 1: Ventral	0	0	1	1
K6: mf8 posterior lobe	0: Fully outwards tilted 1: Little outwards tilted	0	0	1	1
K7: Strong protrusion of the squamosal zygomatic process	0: Absent 1: Present	0	1	0	1
K8: Foramen magnum shape	0: Elliptic 1: Circular 2: Subelliptic	0	1	2	1
K9: Medial concave curvature of descending process of the zygomatic arch	0: Yes 1: No	0	1	1	0
K10: Angle between NFP and POP	0: <170° 1: >170°	0	1	1	0
K11: Orbital shape	0: Circular 1: Subelliptic	0	1	1	0
K12: Largest semicircular canal	0: Anterior and/or posterior 1: Lateral 2: All similar sized	0	0	1	2
K13: Cochlear position	0: Straight 1: Ventrally tilted	0	1	0	1
K14: Cerebrum inclination	0: Dorsal 1: Light ventral	0	0	1	1
K15: Posttemporal canal orientation in lateral view	0: Posteroventral 1: Vertical	0	1	1	?
K16: Orbitotemporal canal course	0: Along braincase lateral wall 1: Passage through cerebrum	0	1	1	?
K17: Distance between optic canal openings	0: Large 1: Small	0	1	0	?

**Fig. 12** (See legend on previous page.)

larger volume of the cerebellum and the smaller volume of the cerebrum while exhibiting an almost inexistent caudal tube (i.e., one or two distal ankylosed bony rings) in comparison with the remaining Pleistocene glyptodont genera (Cuadrelli et al., 2019), indicating a highly armored tail without weaponry. In accordance with the hypothesis of Stankowich & Romero (2017), the smaller volume of the cerebrum of *Glyptodon munizi* might be associated with a more passive defense mode than glyptodonts possessing tails with weaponry, such as *Panochthus* and *Doedicurus*. The major difference concerning the relative volumes of the different parts of the braincase can be found in the relative volume of the olfactory bulb. In *Neosclerocalyptus pseudornatus*, the olfactory bulbs accounts for only 2.4% of the contrary to the 7% in *Glyptodon munizi* and *Doedicurus clavicaudatus* in contrast with extant armadillos for which the olfactory bulbs are large compared to the total volume of the braincase endocast (Tambusso & Fariña, 2015a). In *Neosclerocalyptus pseudornatus* and *Panochthus tuberculatus* (Tambusso & Fariña, 2015a), the olfactory bulbs are more ventrally oriented as mentioned above. According to Tambusso and Fariña (2015a), this ventral orientation could be related to the great development of the paranasal sinuses dorsally to the olfactory bulbs and can be observed in other Hoplophorinae as well, such as *Panochthus tuberculatus* (Tambusso & Fariña, 2015a) and *Neosclerocalyptus paskoensis* (Fernicola et al., 2012). This smaller braincase in cingulates compared to that of extant sloths could be possibly linked to the earlier weaning age (Tambusso & Fariña, 2015a; Weisbecker & Goswami, 2010), the biological, ecological, and locomotory restrictions imposed by the carapace (Lovegrove, 2001), limited defense strategies due to the large body size and carapace (Tambusso & Fariña, 2015a), or the potential low metabolic rate (McNab, 1986, 2008; Vizcaíno et al., 2006). Tambusso and Fariña (2015a) hypothesized a possible link between larger body sizes and a relatively small brain in Pleistocene glyptodonts, a widespread trend among mammals (Burger et al., 2019; Ferreira et al., 2020). Although body size was not estimated in our study, a size gradient from smallest to largest genera appears from *Neosclerocalyptus* to *Doedicurus* (Fariña et al., 1998; Vizcaíno et al., 2011). Consequently, a nearly equivalent braincase endocast raw size between *Glyptodon munizi* and *Doedicurus clavicaudatus* suggest that the relative brain size of the latter is smaller than in other glyptodonts, supporting the hypothesis of Tambusso and Fariña (2015a). Although we mention aspects associated with the relative size of the brain and its units, we did not generate other characters than K14 for the braincase endocast, leaving room for further investigation of the variation of this part of the endocranum and its potential causes.

Besides the brain, for the endocranial anatomy, the potential relation between body mass and semicircular canal relative size observed for glyptodont might be in accordance with the allometric trend suggested by Billet et al. (2015a) for Xenarthra, especially for the relative reduction in size of the lateral semicircular canal when cranial size increase. However, *Neosclerocalyptus pseudornatus* in comparison with *Glyptodon munizi* does not fit clearly this allometric trend. The shape of the semicircular canals in xenarthrans has been hypothesized to be more strongly influenced by phylogeny than by allometry (Billet et al., 2015a). Unlike for extant sloths (Billet et al., 2012, 2015a), other xenarthrans including modern armadillos (Billet et al., 2015a) and extinct glyptodonts (Tambusso et al., 2021) show a low intraspecific variation of the bony labyrinth, which, according to Billet et al. (2012) and Hautier et al. (2014), is possibly related to the relaxation of functional constraints. Based on the shape of the inner ear of the analysed species, a clear difference between *Glyptodon*, *Doedicurus*, *Neosclerocalyptus*, and *Panochthus* was detected, the latter two showing a lateral semicircular canal as the largest or of similar size for all semicircular canals, respectively (K12). The trend of proportionally larger anterior and posterior semicircular canals compared to the lateral semicircular canal in larger species such as *Doedicurus clavicaudatus* compared to the small glyptodont *Neosclerocalyptus pseudornatus* is noteworthy, in particular because K12 supports the alternative phylogenetic hypothesis of Fernicola et al. (2018). According to Billet et al. (2015a), Xenarthra follow a general trend observed in primates and marsupials, where a more ventrally oriented cochlea is displayed in smaller xenarthrans. Our sample contradicts this general trend, with *Doedicurus clavicaudatus* and *Panochthus tuberculatus* (Tambusso et al., 2021) exhibiting the most ventrally oriented cochlea of our sample.

Finally, we compared the patterns of the cranial canals in relation to the braincase (Le Verger et al., 2021). Limited to the available data, in particular because of the lack of information about *Panochthus*, we found that a vertical orientation of the posttemporal canal in lateral view (K15) or a passage of the orbitotemporal canal inside the cranium (K16) could support the clade formed by *Doedicurus*, *Neosclerocalyptus*, and *Panochthus* (Fig. 12), on condition that this hypothesis be confirmed in the latter. These potential endocranial characters might, therefore, preferentially support the phylogenetic hypothesis of Nuñez-Blasco et al. (2021) than that of Fernicola et al. (2018). The circulatory pattern of the orbitotemporal canal appears to be similar between Pleistocene and Miocene glyptodonts (Le Verger et al., 2021), suggesting that *Glyptodon* show a derived pattern of this canal and not a variation due to gigantism. Size variation also does not

seem to explain the convergence we found between *Glyptodon* and *Neosclerocalyptus* with respect to the distance between optic foramina, suggesting a strong derivation in *Doedicurus*. These last results remain to be confirmed while revealing the potential of cranial canals for the systematics of glyptodonts.

The completeness and taxonomic diversity of cranial remains collected by Santiago Roth enables potential studies to improve the understanding of evolution, phylogeny, and taxonomic revisions of glyptodonts of the Pampean Region during the Pleistocene. With this material, we provided novel data on the evolutionary morphology of glyptodonts and highlight the interest of endocranial structures for this purpose. Specifically, we highlighted the equivalent support of potential external cranial characters to two of the most recent evolutionary hypotheses concerning phylogenetic relationships among Pleistocene glyptodont genera and called for further evaluation of certain homological hypotheses, suspecting evolutionary convergences within glyptodonts. As a new insight, we suggested that some endocranial structures could provide answers in the debate opposing the current phylogenetic hypotheses of Pleistocene glyptodonts, encouraging their inclusion in future systematic work. The present work could serve as one of the bases for an extended study of the whole history of the clade.

Acknowledgements

We would like to express our sincere thanks to Gabriel Aguirre Fernández from the PIMUZ, Kasper Lykke Hansen from the ZMK, Lionel Cavin and Edwin Gnos from the MHNG, Antoine Pictet from the MCGL for their hospitality, the access to the collection and the providing of comparative material from the Santiago Roth collection. Furthermore, we would like to thank Jorge Domingo Carrillo Briceño and Alexandra Wegmann from the PIMUZ for the acquisition of the CT scans. We also warmly thank Analía M. Forasiepi from the Instituto Argentino de Nivología, Glaciología y Ciencias Ambientales (CCT-CONICET Mendoza, Argentina), P. Sebastián Tambusso from the Facultad de Ciencias of the Universidad de la República (Montevideo, Uruguay), and Laureano R. González Ruiz from the Centro de Investigación Esquel de Estepa y Montaña Patagónica (CIEMEP) of the Universidad Nacional de la Patagonia San Juan Bosco (UNPSJB—CONICET Esquel, Argentina) for their valuable help in improving the manuscript. Finally, we thank the Swiss National Science Foundation for the financial support of this research.

Author contributions

ZMC conducted the acquisition of data, data interpretations and drafted the manuscript. MRSV contributed to the design of the study and edited the manuscript. KLV supported the data acquisition, designed the study, edited, and revised the manuscript.

Funding

This research was supported by SNF grant IZSTZ0_208545 entitled 'South American Pleistocene Megafaunal Diversification and Extinction—An Evaluation of the Historical Roth collection in Zurich' to MRSV and Analía Forasiepi.

Availability of data and materials

All data related to our comparative investigation are given in the present publication. CT-Scans and Surface scans data on many of the specimens are becoming available in publications concurrent to the present one and the concerned specimens are given in Table 1.

Declaration

Competing interests

The authors declare no competing interests.

Author details

¹Department of Paleontology, University of Zurich, Karl-Schmid-Strasse 4, 8006 Zurich, Switzerland.

Received: 1 February 2023 Accepted: 20 June 2023

Published online: 16 August 2023

References

- Aguirre-Fernández, G., Jost, J., & Hilfiker, S. (2022). First records of extinct kentriodontid and squalodelphinid dolphins from the Upper Marine Molasse (Burdigalian age) of Switzerland and a reappraisal of the Swiss cetacean fauna. *PeerJ*. <https://doi.org/10.7717/peerj.13251>
- Ameghino, F. (1881). *La Antiguedad del Hombre en el Plata 2 Paris G Masson* Buenos Aires. Igon Hermanos.
- Ameghino, F. (1897). II—Notes on the geology and palaeontology of Argentina. *Geological Magazine*, 4(1), 4–20.
- Ameghino, F. (1889). Contribución al conocimiento de los mamíferos fósiles de la República Argentina. *Actas De La Academia Nacional De Ciencias (córdoba)*, 6, 1–1027.
- Ameghino, F. (1908). Las formaciones sedimentarias de la región litoral de Mar del Plata y Chapalmalán. *Anales Del Museo Nacional De Buenos Aires*, 3, 343–428.
- Barnosky, A. D., & Lindsey, E. L. (2010). Timing of Quaternary megafaunal extinction in South America in relation to human arrival and climate change. *Quaternary International*, 217(1–2), 10–29. <https://doi.org/10.1016/j.quaint.2009.11.017>
- Billet, G., De Muizon, C., Schellhorn, R., Ruf, I., Ladèvèze, S., & Bergqvist, L. (2015b). Petrosal and inner ear anatomy and allometry amongst specimens referred to Litopterna (Placentalia). *Zoological Journal of the Linnean Society*, 173(4), 956–987.
- Billet, G., Hautier, L., Asher, R. J., Schwarz, C., Crumpton, N., Martin, T., & Ruf, I. (2012). High morphological variation of vestibular system accompanies slow and infrequent locomotion in three-toed sloths. *Proceedings of the Royal Society B: Biological Sciences*, 279(1744), 3932–3939.
- Billet, G., Hautier, L., de Muizon, C., & Valentin, X. (2011). Oldest cingulate skulls provide congruence between morphological and molecular scenarios of armadillo evolution. *Proceedings of the Royal Society B Biological Sciences*, 278(1719), 2791–2797. <https://doi.org/10.1098/rspb.2010.2443>
- Billet, G., Hautier, L., & Lebrun, R. (2015a). Morphological diversity of the bony labyrinth (inner ear) in extant xenarthrans and its relation to phylogeny. *Journal of Mammalogy*, 96(4), 658–672.
- Boscaini, A., Iurino, D. A., Mamani Quispe, B., Andrade Flores, R., Sardella, R., Pujos, F., & Gaudin, T. J. (2020b). Cranial anatomy and paleoneurology of the extinct sloth *Catonyx taricensis* (Xenarthra, Mylodontidae) from the late Pleistocene of Oruro, Southwestern Bolivia. *Frontiers in Ecology and Evolution*. <https://doi.org/10.3389/fevo.2020.00069>
- Boscaini, A., Iurino, D. A., Sardella, R., Tirao, G., Gaudin, T. J., & Pujos, F. (2020a). Digital cranial endocasts of the extinct sloth *Glossotherium robustum* (Xenarthra, Mylodontidae) from the late Pleistocene of Argentina: Description and comparison with the extant sloths. *Journal of Mammalian Evolution*, 27(1), 55–71.
- Bravard, A. (1857). Geología de las Pampas. *Territorio, Estado Físico Del Territorio, Registro Estadístico Del Estado De Buenos Aires*, 1, 1–22.
- Burger, J. R., George, M. A., Jr., Leadbetter, C., & Shaikh, F. (2019). The allometry of brain size in mammals. *Journal of Mammalogy*, 100(2), 276–283. <https://doi.org/10.1093/jmammal/gyz043>
- Burmeister, G. (1866). Lista de los mamíferos fósiles del terreno diluviano. *Anales Del Museo Público De Buenos Aires*, 1, 121–232.
- Burmeister, G. (1874). Monografía de los glyptodontes en el Museo Público de Buenos Aires. *Anales Del Museo Público De Buenos Aires*, 2, 1–412.
- Butler, A. B., & Hodos, H. (1996). *Comparative vertebrate neuroanatomy: evolution and adaptation*. Wiley-Liss.

- Carlini, A. A., & Scillato-Yané, G. J. (1999). Evolution of Quaternary xenarthrans (Mammalia) of Argentina. In J. Rabassa & M. Salemme (Eds.), *Quaternary vertebrate palaeontology in South America, Quaternary of South America and Antarctic Peninsula*. A. A. Balkema.
- Carlini, A. A., & Zurita, A. E. (2010). An introduction to cingulate evolution and their evolutionary history during the Great American Biotic Interchange: Biogeographical clues from Venezuela. *Urumaco and Venezuelan Paleontology*, 6, 233–255.
- Chichkoyan Kayayan, K. V. (2017). *Initial human dispersal and native fauna at the South American southern cone, Argentina. An example case from the revision of the fossil collections*. (PhD thesis, unpubl.), Doctoral dissertation, Universitat Rovira i Virgili, Departament d’Història i Història de l’Art, Tarragona, Spain. nportal0.urv.cat:18080/fourreppublic/search/item-/TDX%3A2543.
- Cione, A. L., Gasparini, G. M., Soibelzon, E., Soibelzon, L. H., & Tonni, E. P. (2015). *The Great American Biotic Interchange. A South American perspective*. Springer.
- Cione, A. L., & Tonni, E. P. (1995). Chronostratigraphy and “Land-Mammal Ages” in the Cenozoic of southern South America: Principles, practices, and the “Uquian” problem. *Journal of Paleontology*, 69(1), 135–159.
- Cione, A. L., & Tonni, E. P. (1996). Reassessment of the Pliocene-Pleistocene continental time scale of Southern South America. Correlation of the type Chapadmalalan with Bolivian sections. *Journal of South American Earth Sciences*, 9(3–4), 221–236.
- Cione, A. L., & Tonni, E. P. (2005). Bioestratigrafía basada en mamíferos del Cenozoico superior de la provincia de Buenos Aires, Argentina. *Geología y Recursos Minerales De La Provincia De Buenos Aires*, 11, 183–200.
- Cione, A. L., Tonni, E. P., Bond, M., Carlini, A. A., Pardiñas, U. F., Scillato-Yané, G. J., Verzi, D., & Vučetić, M. G. (1999). Occurrence charts of Pleistocene mammals in the Pampean area, eastern Argentina. In E. P. Tonni & A. L. Cione (Eds.), *Quaternary vertebrate palaeontology in South America. Quaternary of South America and Antarctic Peninsula* 12 (pp. 53–59). A. A. Balkema.
- Cope, E. D. (1889). The Edentata of North America. *The American Naturalist*, 23, 657–664.
- Coutier, F., Hautier, L., Cornette, R., Amson, E., & Billet, G. (2017). Orientation of the lateral semicircular canal in Xenarthra and its links with head posture and phylogeny. *Journal of Morphology*, 278(5), 704–717.
- Cuadrelli, F., Zurita, A. E., Toriño, P., Miño-Boilini, Á. R., Perea, D., Luna, C. A., Gillette, D. D., & Medina, O. (2020). A new species of glyptodontine (Mammalia, Xenarthra, Glyptodontidae) from the Quaternary of the Eastern Cordillera, Bolivia: Phylogeny and palaeobiogeography. *Journal of Systematic Palaeontology*, 18(18), 1543–1566. <https://doi.org/10.1080/14772019.2020.1784300>
- Cuadrelli, F., Zurita, A. E., Toriño, P., Miño-Boilini, Á. R., Rodríguez-Bualó, S., Perea, D., & Acuña Suárez, G. E. (2019). Late Pleistocene glyptodontinae (mammalia, xenarthra, glyptodontidae) from southern south America: a comprehensive review. *Journal of Vertebrate Paleontology*. <https://doi.org/10.1080/02724634.2018.1525390>
- Cuvier, G. B. (1958). *Tableau élémentaire de l’histoire naturelle des animaux*. Baudouin imprimeur.
- D’Orbigny, A. (1842). *Voyage dans l’Amérique Méridionale (le Brésil, la République Orientale de l’Uruguay, la République Argentine, la Patagonie, la République du Chili, la République de Bolivie, la République du Pérou)*, exécuté pendant les années 1826, 1827, 1828, 1829, 1830, 1831, 1832 et 1833. Tome Troisième, 4^e Partie: Paléontologie. Paris: P. Bertrand; Strasbourg: V. Levraut.
- Darwin, C.R. (1845). *Journal of researches into the natural history and geology of the countries Visited during the voyage of H.M.S. Beagle round the world, under the command of Capt. Fitz Roy, 2nd ed.* London: R.N. John Murray.
- De Melo França, L., De Asevedo, L., Dantas, M. A. T., Bocchiglieri, A., Dos Santos Avilla, L., Lopes, R. P., & Da Silva, J. L. L. (2015). Review of feeding ecology data of Late Pleistocene mammalian herbivores from South America and discussions on niche differentiation. *Earth-Science Reviews*, 140, 158–165.
- Dechaseaux, C. (1958). *L’encéphale d’Elephas meridionalis*. G. Masson.
- Dechaseaux, C. (1962). Encéfalos de notoungulados y de desdentados xenartros fósiles. *Ameghiniana*, 2(11), 193–209.
- Delsuc, F., Gibb, G. C., Kuch, M., Billet, G., Hautier, L., Southon, J., Rouillard, J. M., Fernicola, J. C., Vizcaíno, S. F., MacPhee, R. D. E., & Poinar, H. N. (2016). The phylogenetic affinities of the extinct glyptodonts. *Current Biology*, 26(4), R155–R156. <https://doi.org/10.1016/j.cub.2016.01.039>
- Deschamps, C. M., & Tomassini, R. L. (2016). *Late Cenozoic vertebrates from the southern Pampean Region systematic and bio-chronostratigraphic update*. Publicación Electrónica de la Asociación Paleontológica Argentina (PE-APA). <https://doi.org/10.5710/PEPA.16.05.2016.113>
- Domingo, L., Prado, J. L., & Alberdi, M. T. (2012). The effect of paleoecology and paleobiogeography on stable isotopes of Quaternary mammals from South America. *Quaternary Science Reviews*, 55, 103–113.
- Dozo, M. T. (1998). Neuromorfología de *Utaetus buccatus* (Xenarthra, Dasypodidae): Un armadillo del Eoceno temprano de la Provincia del Chubut Argentina. *Ameghiniana*, 35(3), 285–289.
- Evans, H. E., & De Lahuta, A. (2012). *Miller’s Anatomy of the Dog*. Saunders.
- Fariña, R. A. (1995). Limb bone strength and habits in large glyptodonts. *Lethaia*, 28(3), 189–196.
- Fariña, R. A., Vizcaíno, S. F., & Bargo, M. S. (1998). Body mass estimations in Lujanian (late Pleistocene–early Holocene of South America) mammal megafauna. *Mastozoología Neotropical*, 5(2), 87–108.
- Fernicola, J. C. (2008). Nuevos aportes para la sistemática de los Glyptodontia Ameghino 1889 (Mammalia, Xenarthra, Cingulata). *Ameghiniana*, 45(3), 553–574.
- Fernicola, J. C., & Porpino, K. D. O. (2012). Exoskeleton and systematics: A historical problem in the classification of glyptodonts. *Journal of Mammalian Evolution*, 19(3), 171–183.
- Fernicola, J. C., Rinderknecht, A., Jones, W., Vizcaíno, S. F., & Porpino, K. (2018). A new species of *Neoglyptelus* (Mammalia, Xenarthra, Cingulata) from the late Miocene of Uruguay provides new insights on the evolution of the dorsal armor in cingulates. *Ameghiniana*, 55(3), 233–252. <https://doi.org/10.5710/AMGH.02.12.2017.3150>
- Fernicola, J. C., Toledo, N., Bargo, S., & Vizcaíno, S. F. (2012). A neomorphic ossification of the nasal cartilages and the structure of paranasal sinus system of the glyptodont *Neosclerocalyptus* Paula Couto 1957 (Mammalia, Xenarthra). *Palaeontología Electrónica*. <https://doi.org/10.26879/333>
- Ferreira, J. D., Negri, R. F., Sánchez-Villagra, M. R., & Kerber, L. (2020). Small within the largest: Brain size and anatomy of the extinct *Neopiblema acrensis*, a giant rodent from the Neotropics. *Biology Letters*, 16(2), 20190914.
- Gaudin, T. J., & Lyon, L. M. (2017). Cranial osteology of the pampatheres *Holmesina floridanus* (Xenarthra: Cingulata; Blanca NALMA), including a description of an isolated petrosal bone. *PeerJ*. <https://doi.org/10.7717/peerj.4022>
- Gaudin, T. J., & Wible, J. R. (2006). The phylogeny of living and extinct armadillos (Mammalia, Xenarthra, Cingulata): A craniodental analysis. In M. T. Carrano, T. J. Gaudin, R. W. Blob, & J. R. Wible (Eds.), *Amniote paleobiology: Perspectives on the evolution of mammals, birds, and reptiles* (pp. 153–198). University of Chicago Press.
- Gervais, H., & Ameghino, F. (1880). *Los mamíferos fósiles de la América del Sur*. Sabih & Igon.
- Gervais, P. (1869). *Zoologie et paléontologie générales* (Vol. 1). Arthus Bertrand.
- Gillette, D. D., & Ray, C. E. (1981). Glyptodonts of North America. *Smithsonian Contributions on Paleobiology*, 4, 1–255.
- González-Ruiz, L. R., Ciancio, M. R., Martin, G. M., & Zurita, A. E. (2015). First record of supernumerary teeth in Glyptodontidae (Mammalia, Xenarthra, Cingulata). *Journal of Vertebrate Paleontology*. <https://doi.org/10.1080/02724634.2014.885033>
- Gray, J. E. (1869). Catalogue of carnivorous, pachydermatous, and edentate Mammalia in the British Museum. British Museum.
- Guth, C. (1961). *La région temporelle des Édentés*. Le Puy: impr. Jeanne d’Arc.
- Hansen, K.L. (2019). *From the shadows out of time*. (PhD thesis, unpubl.), University of Copenhagen, Faculty of Science, Copenhagen, Denmark. [https://globe.ku.dk/staff-list/?pure=en%2Fpublications%2Ffrom-the-shadows-out-of-time\(64149b17-30b4-4197-8fd3-cdfc39e8a184\).html](https://globe.ku.dk/staff-list/?pure=en%2Fpublications%2Ffrom-the-shadows-out-of-time(64149b17-30b4-4197-8fd3-cdfc39e8a184).html).
- Hautier, L., Billet, G., Eastwood, B., & Lane, J. (2014). Patterns of morphological variation of extant sloth skulls and their implication for future conservation efforts. *The Anatomical Record*, 297(6), 979–1008.
- Heesy, C. P. (2004). On the relationship between orbit orientation and binocular visual field overlap in mammals. *The Anatomical Record*, 281(1), 1104–1110.
- Heesy, C. P. (2008). Ecomorphology of orbit orientation and the adaptive significance of binocular vision in primates and other mammals. *Brain, Behavior and Evolution*, 71(1), 54–67.
- Huxley, T. H. (1864). On the osteology of the genus *Glyptodon*. *Proceedings of the Royal Society of London*, 13(1864), 108–108.

- Illiger, J. K. W. (1811). *Prodromus Systematis Mammalium et Avium: Additis Terminis Zoographicis Utriusque Classis, Eorumque Versione Germanica* (p. 301). Salfeld C.
- Le Verger, K. (2023). Xenarthrans of the collection of Santiago Roth from the Pampean Region of Argentina (Pleistocene), in Zurich. Switzerland. *Swiss Journal of Palaeontology*, 142(3), 1–39. <https://doi.org/10.1186/s13358-023-00265-7>
- Le Verger, K., González Ruiz, L. R., & Bille, G. (2021). Comparative anatomy and phylogenetic contribution of intracranial osseous canals and cavities in armadillos and glyptodonts (Xenarthra, Cingulata). *Journal of Anatomy*, 239(6), 1473–1502.
- Le Verger, K., Hautier, L., Bardin, J., Gerber, S., Delsuc, F., & Bille, G. (2020). Ontogenetic and static allometry in the skull and cranial units of nine-banded armadillos (Cingulata: Dasypodidae: *Dasypus novemcinctus*). *Biological Journal of the Linnean Society*, 131(3), 673–698.
- Linnaeus, C. (1758). *Systema naturae per regna tria naturae, secundum classes, ordines, genera, species, cum characteribus, differentiis, synonymis, locis. Tomus I. Editio decima, reformata. Homiae: Laurentii Salvii.*
- Lovegrove, B. (2001). The evolution of body armor in mammals: Plantigrade constraints of large body size. *Evolution*, 55, 1464–1473.
- Lund, P. W. (1839). Blik paa Brasiliens dyreverden for sidste jordomvæltning. Anden afhandling: Pattedyrene. *Det Kongelige Danske Videnskabernes Selskabs Naturvidenskabelige Og Mathematiske Afhandlinger*, 8, 61–144.
- Lydekker, R. (1894). *The royal natural history* (Vol. 1). Frederick Warne & Co.
- Lydekker, R. (1895). Contributions to a knowledge of the fossil vertebrates of Argentina. The extinct edentates of Argentina. *Anales Del Museo De La Plata, Paleontología Argentina*, 3, 1–118.
- MacPhee, R. D., Del Pino, S. H., Kramarz, A., Forasiepi, A. M., Bond, M., & Sulser, R. B. (2021). Cranial morphology and phylogenetic relationships of *Trigonostylops wortmani*, an Eocene South American native ungulate. *Bulletin of the American Museum of Natural History*, 449(1), 1–183. <https://doi.org/10.1206/0003-0090.449.1.1>
- McKenna, M. C., & Bell, S. K. (1997). *Classification of mammals: Above the species level*. Columbia University Press.
- McNab, B. K. (1986). The influence of food habits on the energetics of eutherian mammals. *Ecological Monographs*, 56(1), 1–19.
- McNab, B. K. (2008). An analysis of the factors that influence the level and scaling of mammalian BMR. *Comparative Biochemistry and Physiology Part a: Molecular & Integrative Physiology*, 151(1), 5–28.
- Mitchell, K. J., Scanferla, A., Soibelzon, E., Bonini, R., Ochoa, J., & Cooper, A. (2016). Ancient DNA from the extinct South American giant glyptodont *Doedicurus* sp. (Xenarthra: Glyptodontidae) reveals that glyptodonts evolved from Eocene armadillos. *Molecular Ecology*, 25(14), 3499–3508.
- Navel, P., Cione, A., & Tonni, P. (2000). Environmental changes in the Pampean area of Argentina at the Matuyama-Brunhes (C1r–C1n) Chrons boundary. *Palaeogeography Palaeoclimatology Palaeoecology*, 162, 403–412.
- Núñez-Blasco, A., Zurita, A. E., Miño-Boilini, Á. R., Bonini, R. A., & Cuadrelli, F. (2021). The glyptodont *Eleutherocercus solidus* from the late Neogene of north-western Argentina: Morphology, chronology, and phylogeny. *Acta Palaeontologica Polonica*, 66(3), 80–99.
- Osborn, H. F. (1903). *Glyptotherium Texanum*: A New Glyptodont from the Lower Pleistocene of Texas. *Bulletin of the American Museum of Natural History*, 19, 491–494.
- Owen, R. (1839a). Description of a tooth and part of the skeleton of the *Glyptodon*, a large quadruped of the edentate order, to which belongs the tessellated bony armour figured by Mr Clift in his memoir on the remains of the *Megatherium*, brought to England by Sir Woodbine Parish, F.G.S. *Proceedings of the Geological Society of London*, 3, 108–113.
- Owen, R. (1839b). *Zoology of the Voyage of the Beagle, under the command of Captain Fitzroy R.N., during the years 1832–1826 Part 1 Fossil Mammalia. Elder and Co.*
- Owen, R. (1845). *Descriptive and illustrated catalogue of the fossil organic remains of Mammalia and Aves contained in the Museum of the Royal College of Surgeons of London, England*. R. & J.E. Taylor.
- Pardiñas, U. F., & Deschamps, C. (1996). Sigmodontinos (Mammalia, Rodentia) pleistocénicos del sudeste de la provincia de Buenos Aires (Argentina): Aspectos sistemáticos, paleozoogeográficos y paleoambientales. *Estudios Geológicos*, 52(5–6), 367–379.
- Paula Couto, C. (1957). Sobre um gliptodonte do Brasil. Rio de Janeiro. *Boletim Divisão De Geologia e Mineralogia*, 165, 1–37.
- Porpino, K. D. O., Fernicola, J. C., & Bergqvist, L. P. (2010). Revisiting the intertropical Brazilian species *Hoplophorus euphractus* (Cingulata, Glyptodontidae) and the phylogenetic affinities of *Hoplophorus*. *Journal of Vertebrate Paleontology*, 30(3), 911–927.
- Prado, J. L., Alberdi, M. T., & Bellinzoni, J. (2021). Pleistocene mammals from Pampean Region (Argentina). Biostatigraphic, biogeographic, and environmental implications. *Quaternary*, 4(2), 15.
- Prado, J. L., Martínez-Maza, C., & Alberdi, M. T. (2015). Megafauna extinction in South America: A new chronology for the Argentine Pampas. *Palaeogeography Palaeoclimatology Palaeoecology*, 425, 41–49.
- Prado, J. L., Sánchez, B., & Alberdi, M. T. (2011). Ancient feeding ecology inferred from stable isotopic evidence from fossil horses in South America over the past 3 Ma. *BMC Ecology*, 11, 15. <https://doi.org/10.1186/1472-6785-11-15>
- Prevosti, F. J., & Forasiepi, A. M. (2018). *Evolution of South American Mammalian Predators during the cenozoic: Paleoibiogeographic and paleoenvironmental contingencies*. Springer.
- Quattrochio, M. E., Borromei, A. M., Deschamps, C. M., Grill, S. C., & Zavala, C. A. (2008). Landscape evolution and climate changes in the late pleistocene-holocene, southern pampa (Argentina): Evidence from palynology, mammals and sedimentology. *Quaternary International*, 181(1), 123–138.
- Quiñones, S. I., Reyes los De, M., Zurita, A. E., Cuadrelli, F., Miño-Boilini, A. R., & Poire, D. G. (2020). *Neosclerocalyptus Paula Couto* (Xenarthra, Glyptodontidae) in the late pliocene–earliest pleistocene of the pampean region (Argentina): Its contribution to the understanding of evolutionary history of Pleistocene glyptodonts. *Journal of South American Earth Sciences*, 103, 102701. <https://doi.org/10.1016/j.jsames.2020.102701>
- Rabassa, J., & Coronato, A. (2009). Glaciations in patagonia and tierra del fuego during the ensenadan stage/age (early Pleistocene–earliest middle Pleistocene). *Quaternary International*, 210(1–2), 18–36.
- Rabassa, J., Coronato, A. M., & Salemme, M. (2005). Chronology of the late cenozoic patagonian glaciations and their correlation with biostatigraphic units of the Pampean Region (Argentina). *Journal of South American Earth Sciences*, 20(1–2), 81–103.
- Riggi, J., Hidalgo, F., Martínez, O., & Porro, N. (1986). Geología de los “Sedimentos Pampeanos” en el Partido de La Plata. *Revista De La Asociación Geológica Argentina*, 41, 316–333.
- Robertson, J. S. (1976). Latest Pliocene mammals from Haile XV A, Alachua County, Florida. *Bulletin of the Florida State Museum Biological Sciences*, 20(3), 111–186.
- Roth, S. (1889). *Fossiles de La Pampa, Amérique du Sud, collectionnés par Santiago Roth Catalogue*. Jean Meyer.
- Sánchez-Villagra, M. R., Bond, M., Reguero, M., & Bartoletti, T. J. (2023). From fossil trader to palaeontologist: On Swiss-born naturalist Santiago Roth and his scientific contributions. *Swiss Journal of Palaeontology*, 142, 8.
- Schade, M., Stumpf, S., Kriwet, J., Kettler, C., & Pfaff, C. (2022). Neuroanatomy of the nodosaurid *Struthiosaurus austriacus* (Dinosauria: Thyreophora) supports potential ecological differentiations within Ankylosauria. *Scientific Reports*, 12(1), 1–9.
- Schluthess, B. (1920). *Beiträge zur Kenntnis der Xenarthra auf Grund der Santiago Roth'schen Sammlung des Zoologischen Museums der Universität Zürich*. Albert Kundig.
- Soibelzon, E. (2019). Using paleoclimate and the fossil record to explain past and present distributions of armadillos (Xenarthra, Dasypodidae). *Journal of Mammalian Evolution*, 26(1), 61–70.
- Soibelzon, E., Prevosti, F. J., Bidegain, J. C., Rico, Y., Verzi, D. H., & Tonni, E. P. (2009). Correlation of late Cenozoic sequences of southeastern Buenos Aires province: Biostatigraphy and magnetostratigraphy. *Quaternary International*, 210(1–2), 51–56.
- Soibelzon, E., Zurita, A. E., & Carlini, A. A. (2006). *Glyptodon munizi Ameghino* (Mammalia, Cingulata, Glyptodontidae): Redescripción y anatomía. *Ameghiniana*, 43(2), 377–384.
- Soibelzon, L. H., Rinderknecht, A., Tarquini, J., & Ugalde, R. (2019). First record of fossil procyonid (Mammalia, Carnivora) from Uruguay. *Journal of South American Earth Sciences*, 92, 368–373.
- Stankowich, T., & Romero, A. N. (2017). The correlated evolution of antipredator defences and brain size in mammals. *Proceedings of the Royal Society B Biological Sciences*, 284(1846), 20161857. <https://doi.org/10.1098/rspb.2016.1857>

- Sultan, F., & Glickstein, M. (2007). The cerebellum: Comparative and animal studies. *The Cerebellum*, 6(3), 168–176.
- Tambusso, P. S., & Fariña, R. A. (2015a). Digital cranial endocast of *Pseudoplophorus absolutus* (Xenarthra, Cingulata) and its systematic and evolutionary implications. *Journal of Vertebrate Paleontology*, 35(5), e967853. <https://doi.org/10.1080/02724634.2015.967853>
- Tambusso, P. S., Góis, F., Moura, J. F., Villa, C., & Amaral do, R. V. (2023). Paleoneurology of extinct cingulates and insights into their inner ear anatomy. In M. T. Dozo, A. Paulina-Carabajal, T. E. Macrini, & S. Walsh (Eds.), *Paleoneurology of amniotes: New directions in the study of fossil endocasts* (pp. 711–736). Springer International Publishing.
- Tambusso, P. S., Varela, L., Góis, F., Moura, J. F., Villa, C., & Fariña, R. A. (2021). The inner ear anatomy of glyptodonts and pampatheres (Xenarthra, Cingulata): Functional and phylogenetic implications. *Journal of South American Earth Sciences*, 108, 103189. <https://doi.org/10.1016/j.jsames.2021.103189>
- Tambusso, S. P., & Fariña, R. A. (2015b). Digital endocranial cast of *Pampatherium humboldtii* (Xenarthra, Cingulata) from the Late Pleistocene of Uruguay. *Swiss Journal of Palaeontology*, 134(1), 109–116.
- Tonni, E. P., Alberdi, M. T., Prado, J., Bargo, M. S., & Cione, A. L. (1992). Changes of mammal assemblages in the pampean region (Argentina) and their relation with the Plio-Pleistocene boundary. *Palaeogeography Palaeoclimatology Palaeoecology*, 95(3–4), 179–194.
- Tonni, E. P., Nabel, P., Cione, A. L., Etchichury, M., Tófalo, R., Yané, S. G., San Cristóbal, J., Carlini, A. A., & Vargas, D. (1999). The ensenada and buenos aires formations (Pleistocene) in a quarry near la plata, argentina. *Journal of South American Earth Sciences*, 12(3), 273–291.
- Trouessart, E. L. (1897). *Catalogus mammalium tam viventium quam fossilium*. R. Friedländer & sohn.
- Van Essen, D. C. (1979). Visual areas of the mammalian cerebral cortex. *Annual Review of Neuroscience*, 2(1), 227–261.
- Varela, L., & Fariña, R. A. (2016). Co-occurrence of mylodontid sloths and insights on their potential distributions during the late Pleistocene. *Quaternary Research*, 85(1), 66–74.
- Varela, L., Tambusso, P. S., & Patiño, S. J. (2018). Potential distribution of fossil xenarthrans in South America during the Late Pleistocene: Co-occurrence and provincialism. *Journal of Mammalian Evolution*, 25, 539–550. <https://doi.org/10.1007/s10914-017-9406-9>
- Verzi, D. H., Deschamps, C. M., & Tonni, E. P. (2004). Biostratigraphic and paleoclimatic meaning of the Middle Pleistocene South American rodent *Ctenomys kraglievichi* (Caviomorpha, Octodontidae). *Palaeogeography Palaeoclimatology Palaeoecology*, 212, 315–329.
- Verzi, D. H., & Lezcano, M. (1996). Status sistemático y antigüedad de *Megactenomys kraglievichi* Rusconi, 1930 (Rodentia, Octodontidae). *Revista Del Museo De La Plata*, 9(60), 239–246.
- Vizcaíno, S. F., Bargo, M. S., & Cassini, G. H. (2006). Dental occlusal surface area in relation to body mass, food habits and other biological features in fossil xenarthrans. *Ameghiniana*, 43(1), 11–26.
- Vizcaíno, S. F., Cassini, G. H., Fernicola, J. C., & Bargo, M. S. (2011). Evaluating habitats and feeding habits through ecomorphological features in glyptodonts (Mammalia, Xenarthra). *Ameghiniana*, 48(3), 305–319.
- Vizcaíno, S.F., Cassini, G.H., Toledo, N., Bargo, M.S., Patterson, B.P., & Costa, L.P. (2012). On the evolution of large size in mammalian herbivores of Cenozoic. *Bones, clones and biomes: an*, 76–101.
- Vizcaíno, S. F., Fariña, R. A., Bargo, M. S., & De Iuliis, G. (2004). Functional and phylogenetic assessment of the masticatory adaptations in Cingulata (Mammalia, Xenarthra). *Ameghiniana*, 41(4), 651–664.
- Vizcaíno, S. F., & Loughry, W. J. (2008). *Biology of the Xenarthra*. University Press of Florida.
- Voglino, D., Carrillo-Briceño J.D., Furrer H., Balcarcel A., Rangel De Lazaro G., Fernandez G.A., & Forasiepi A.M. 2023. Pampean megamammals in Europe: The fossil collections from Santiago Roth. *Swiss Journal of Palaeontology*.
- Voglino, D. (2020). *Sitios geológicos y paleontológicos estudiados por Santiago Roth en el centro-este de la Argentina*. Museo de Ciencias Naturales P Antonio Scasso.
- Weisbecker, V., & Goswami, A. (2010). Brain size, life history, and metabolism at the marsupial/placental dichotomy. *Proceedings of the National Academy of Sciences*, 107(37), 16216–16221.
- Wible, J. R. (2010). Petrosal anatomy of the nine-banded armadillo, *Dasyurus novemcinctus* Linnaeus, 1758 (Mammalia, Xenarthra, Dasypodidae). *Annals of Carnegie Museum*, 79(1), 1–28.
- Wible, J. R., & Gaudin, T. J. (2004). On the cranial osteology of the yellow armadillo *Euphractus sexcinctus* (Dasypodidae, Xenarthra, Placentalia). *Annals of the Carnegie Museum Pittsburgh*, 73, 117–117.
- Zamorano, M., & Brandoni, D. (2013). Phylogenetic analysis of the Panochthini (Xenarthra, Glyptodontidae), with remarks on their temporal distribution. *Alcheringa an Australasian Journal of Palaeontology*, 37(4), 442–451.
- Zamorano, M., Scillato, G. J., & Zurita, A. E. (2014a). Revisión del género *Panochthus* (Xenarthra, Glyptodontidae). *Revista Museo La Plata Sección Paleontología*, 14, 1–46.
- Zamorano, M., Soibelzon, E., & Tonni, E. P. (2021). Giants of the pampean plains (Argentina) during Early Pleistocene (Ensenadan). The case of *Panochthus* (Xenarthra, Glyptodontidae): Comparative descriptions. *Neues Jahrbuch Für Geologie Und Paläontologie-Abhandlungen*, 302(1), 35–51. <https://doi.org/10.1127/njpa/2021/1017>
- Zamorano, M., Taglioretti, M., Zurita, A. E., Scillato Yané, G. J., & Scaglia, Y. F. (2014b). *El registro más antiguo de Panochthus (Xenarthra Estudios Geológicos Glyptodontidae)*. *Estudios Geológicos*. <https://doi.org/10.3989/egeol.41443.289>
- Zurita, A. E. (2002). Nuevo gliptodonte (Mammalia, Glyptodontidae) del Cuaternario de la provincia de Chaco(Argentina). *Ameghiniana*, 39(2), 175–182.
- Zurita, A. E. (2007). *Sistemática y evolución de los Hoplophorini (Xenarthra: Glyptodontidae: Hoplophorinae). Mioceno tardío–Holoceno temprano*. (PhD thesis, unpubl.), Universidad Nacional de La Plata. Facultad de Ciencias Naturales y Museo, Programa de Doctor en Ciencias Naturales, La Plata, Argentina. <http://naturalis.fcnym.unlp.edu.ar/id/20120126000008>.
- Zurita, A. E., Carlini, A. A., & Scillato Yané, G. J. (2008). A new species of *Neosclerocalyptus* Paula Couto, 1957 (Xenarthra, Glyptodontidae, Hoplophorinae) from the middle Pleistocene of the Pampean Region Argentina. *Geodiversitas*, 30(4), 779–791. <https://doi.org/10.5167/uzh-9473>
- Zurita, A. E., Gillette, D. D., Cuadrelli, F., & Carlini, A. A. (2018). A tale of two clades: Comparative study of *Glyptodon* Owen and *Glyptotherium* Osborn (Xenarthra, Cingulata, Glyptodontidae). *Geobios*, 51(3), 247–258.
- Zurita, A. E., Gonzalez Ruiz, L. R., Gómez-Cruz, A. J., & Arenas-Mosquera, J. E. (2013). The most complete known Neogene Glyptodontidae (Mammalia, Xenarthra, Cingulata) from northern South America: Taxonomic, paleobiogeographic, and phylogenetic implications. *Journal of Vertebrate Paleontology*, 33(3), 696–708.
- Zurita, A. E., Oliveira, E. V., Torriño, P., Rodríguez-Bualó, S. M., Scillato-Yané, G. J., Luna, C. A., & Krapovickas, J. (2011a). On the taxonomic status of some Glyptodontidae (Mammalia, Xenarthra, Cingulata) from the Pleistocene of South America. *Annales De Paleontologie*, 97(1), 63–83. <https://doi.org/10.1016/j.anpal.2011.07.003>
- Zurita, A. E., Scarano, A. C., Carlini, A. A., Scillato-Yané, G. J., & Soibelzon, E. (2011b). *Neosclerocalyptus* spp (Cingulata: Glyptodontidae: Hoplophorini): Cranial morphology and palaeoenvironments along the changing Quaternary. *Journal of Natural History*, 45(15–16), 893–914. <https://doi.org/10.1080/00222933.2010.536917>
- Zurita, A. E., Scillato-Yané, G. J., Ciancio, M., Zamorano, M., & González Ruiz, L. R. (2016). Los Glyptodontidae (Mammalia, Xenarthra): Historia biogeográfica y evolutiva de un grupo particular de mamíferos acorazados. *Historia Evolutiva y Paleobiogeográfica De Los Vertebrados De América Del Sur*, 6, 249–262.
- Zurita, A. E., Taglioretti, M., De Reyes los, R. M., Oliva, C., & Scaglia, F. (2014). First Neogene skulls of *Doedicurinae* (Xenarthra, Glyptodontidae): Morphology and phylogenetic implications. *Historical Biology*, 28, 423–432.
- Zurita, A. E., Zamorano, M., Scillato-Yané, G. J., Fidel, S., Iriondo, M., & Gillette, D. D. (2017). A new species of *Panochthus* Burmeister (Xenarthra, Cingulata, Glyptodontidae) from the Pleistocene of the Eastern Cordillera Bolivia. *Historical Biology*, 29(8), 1076–1088.

Publisher's Note

Springer Nature remains neutral with regard to jurisdictional claims in published maps and institutional affiliations.